Density functional study of multiplicity-changing valence and Rydberg excitations of p-block elements: Delta self-consistent field, collinear spin-flip time-dependent density functional theory (DFT), and conventional time-dependent DFT

Ke Yang,[1] Roberto Peverati,[1] Donald G. Truhlar,[1,a)] and Rosendo Valero[2]
[1]*Department of Chemistry and Supercomputing Institute, University of Minnesota, 207 Pleasant Street S.E., Minneapolis, MN 55455-0431, USA*
[2]*Molecular Physical Chemistry Group, Department of Chemistry, University of Coimbra, 3004-535 Coimbra, Portugal*

(Received 9 May 2011; accepted 14 June 2011; published online 28 July 2011)

A database containing 17 multiplicity-changing valence and Rydberg excitation energies of p-block elements is used to test the performance of density functional theory (DFT) with approximate density functionals for calculating relative energies of spin states. We consider only systems where both the low-spin and high-spin state are well described by a single Slater determinant, thereby avoiding complications due to broken-symmetry solutions. Because the excitations studied involve a spin change, they require a balanced treatment of exchange and correlation, thus providing a hard test for approximate density functionals. We test three formalisms for predicting the multiplicity-changing transition energies. First is the ΔSCF method; we also test time-dependent density functional theory (TDDFT), both in its conventional form starting from the low-spin state and in its collinear spin-flip form starting from the high-spin state. Very diffuse basis functions are needed to give a qualitatively correct description of the Rydberg excitations. The scalar relativistic effect needs to be considered when quantitative results are desired, and we include it in the comparisons. With the ΔSCF method, most of the tested functionals give mean unsigned errors (MUEs) larger than 6 kcal/mol for valence excitations and MUEs larger than 3 kcal/mol for Rydberg excitations, but the performance for the Rydberg states is much better than can be obtained with time-dependent DFT. It is surprising to see that the long-range corrected functionals, which have 100% Hartree–Fock exchange at large inter-electronic distance, do not improve the performance for Rydberg excitations. Among all tested density functionals, ΔSCF calculations with the O3LYP, M08-HX, and OLYP functionals give the best overall performance for both valence and Rydberg excitations, with MUEs of 2.1, 2.6, and 2.7 kcal/mol, respectively. This is very encouraging since the MUE of the CCSD(T) coupled cluster method with quintuple zeta basis sets is 2.0 kcal/mol; however, caution is advised since many popular density functionals give poor results, and there can be very significant differences between the ΔSCF predictions and those from TDDFT. © *2011 American Institute of Physics*. [doi:10.1063/1.3607312]

I. INTRODUCTION

Density functional theory (DFT) is the most robust and widely used electronic structure method in quantum chemistry and solid-state physics. It is a formally exact many-body quantum theory for ground states.[1] Most of the practical applications employ the Kohn-Sham formalism,[2] which is based on a noninteracting reference system, represented by a single Slater determinant that yields the ground-state density of the real system, and on an unknown functional of the electron density; the latter is called the exchange-correlation (xc) functional. In real applications of DFT, one needs to approximate the unknown exchange-correlation functional. Many approximate xc functionals have been developed, and they are reviewed in a recent review.[3] The reliability of the approximate xc functionals is best determined by validation studies against experimental or high-level wave function results. It is generally agreed that, with currently available xc functionals, DFT works best for systems that can be well represented by a single Slater determinant.[4–6]

Density functional theory was originally designed for ground-state properties. In many cases, we are interested in excited-state properties, such as excitation energies. Two approaches have been introduced to calculate the excitation energy with DFT. One approach is called the ΔSCF scheme; it obtains the excitation energy from two Kohn–Sham self-consistent-field (SCF) calculations, one for the ground state and one for the excited state. This approach, in general, is not formally justified. However, for an excited state that is the lowest-energy state with a specified symmetry, the ΔSCF approach has been justified by Gunnarsson and Lundqvist.[7] A difficulty with this approach is that the correct xc functional for excited states depends on the symmetry, although one usually uses the same xc approximations as were originally

a)Author to whom correspondence should be addressed. Electronic mail: truhlar@umn.edu.

designed for the ground state, which is reasonable only for a subset of the excited states.[4–6]

Another approach is to consider the response of the Kohn–Sham ground state to an external time-dependent potential by time-dependent density functional theory (TDDFT).[8–13] The theoretical foundation of TDDFT has been presented and critiqued elsewhere.[12–16] In this article we are only concerned with calculating linear response by TDDFT; linear-response TDDFT may be considered as a correlation-corrected version of linear response time-dependent Hartree–Fock theory.[13,17] Practical applications of linear-response TDDFT usually employ the adiabatic approximation, by which the xc functional is independent of frequency, and it is usually taken to be the same as one of the xc approximations originally developed for the static ground state.[10–13]

For multiplicity-changing transitions, adiabatic linear-response TDDFT calculations, which will just be called TDDFT in the rest of this article, can be carried out in two ways, either starting from the low-spin state or starting from the high-spin state. The former, which is the conventional approach, will be called low-spin TDDFT (LS-TDDFT), and the latter will be called spin-flip TDDFT (SF-TDDFT). Low-spin TDDFT describes the singlet–triplet excitations from a closed-shell singlet ground state to the $M_S = 0$ component of the triplet; however, the errors are larger than those for singlet-singlet excitations.[18] For systems with an even number of electrons, one can calculate both the singlet and the $M_S = 0$ triplet as spin flips from a high-spin $M_S = 1$ triplet by SF-TDDFT.[19,20] The high-spin state is then called the reference state. Likewise, for systems with odd number of electrons, doublet–quartet splittings can be calculated, since both the doublet and the $M_S = 1/2$ quartet can be obtained as spin flips from a high-spin, $M_S = 3/2$ quartet.[21] The SF-TDDFT method was designed to access electronic states such as ground-state open-shell singlet diradicals that cannot be represented in the conventional TDDFT formulation, which only includes single excitations from a closed-shell state.[22] However, SF-TDDFT can also be used to calculate singlet–triplet splittings for systems that are closed-shell singlets in their ground state and to calculate doublet–quartet splittings for systems that are doublets with a single unpaired electron in their ground state, and it is for these purposes that we apply the formalism in the present work. An advantage of the spin-flip technique is that it can include doubly excited configurations since they may be generated by a single-electron transition from the initial state that is already singly excited.[23] The SF-TDDFT has been applied to polyene systems, and uniformly good performance were obtained for excited states with single, double, or mixed excitation character.[24] Both collinear[19] and noncollinear[20] versions of SF-TDDFT have been proposed, but here we consider only the collinear version.

The SF-TDDFT strategy has already been applied to several problems in chemistry, such as the study of the diradical character and singlet–triplet splittings of organic systems[25–28] and the study of organic triradicals,[21] bioinorganic chemistry,[29–32] conical intersections,[33,34] and electron transfer couplings.[35–37]

Multiplicity-changing excitation energies are of special interest for transition metals, which have many spin states with very small energy differences. The accurate description of the energy differences between spin states is also crucial for a correct description of reaction mechanisms.[38] Different spin states of the same compound may have different reactivity, and the spin states may change during the reaction, which leads to the important "two-state reactivity" concept in organometallic chemistry.[39] Spin-crossover complexes, where two spin states have a small energy difference comparable to thermal energy and can be changed by temperature, pressure, irradiation, external magnetic changes, or ligand substitution, have attracted considerable attention in the inorganic chemistry community with a variety of potential applications.[40–42] For many interesting systems, DFT might be the only potentially reliable approach to include correlation effects, since the molecules may be too large for reliable wave function methods. However, the correct calculation of the energy differences between spin states is a very challenging theoretical problem.[43] Validation studies of the high-spin/low-spin energy splitting of transition metal complexes, mainly iron complexes, have been carried out to determine the accuracy of approximate density functionals for spin splitting.[44–58] A functional with reduced percentage of Hartree–Fock exchange, denoted as B3LYP*, was developed with the aim of improving the performance for spin splitting.[44] Several of the validation studies[50–52,54–58] show excellent performance for the OPBE,[59,60] OLYP,[59,61] and TPSSh functionals[62] for spin splitting.

Predicting spin splittings accurately with DFT is very difficult because it requires a balanced treatment of exchange and correlation. Exchange favors the high-spin states and correlation favors the low-spin states, which have more electron repulsion.[3,63] To make the situation even more challenging, the low-spin states often cannot be well described by a single Slater determinant, and a SCF calculation with approximate xc functionals will often lead to a broken symmetry (BS) solution with localized unpaired spins as the lowest energy solution. Various approaches have been used to extract the spin splitting energy from broken-symmetry solutions,[4,5,64–67] and the broken-symmetry approach has been shown to be quite successful with the current approximate functionals.[3,63] One can, however, question the appropriateness of BS approaches by pointing out that "the BS solutions are formally artifacts of our approximate exchange-correlation functionals."[68] If we attempt to test the reliability of approximate functionals for spin splitting, our conclusions are inevitably tempered by the fact that we have two significant sources of errors: (i) the approximation of the BS formalism or whatever other method is used to extract the excitation energy from the calculations; (ii) the approximate character of the tested functionals. *A key strategic element of the present article is that we only consider systems where both the low-spin and high-spin states can be well represented by a Slater determinant, and thereby we avoid having to use BS solutions.* So we will be better able to isolate and study the second kind of error, namely, the intrinsic deficiency of the approximate functionals.

Due to the lack of reliable experimental results for many molecules of interest, many DFT validation studies in the

literature were performed by comparing DFT predictions to results obtained with wave function calculations employing second-order perturbation theory based on a complete-active-space reference wave function (CASPT2).[69,70] The uncertainty of CASPT2 reference results can be up to 3 kcal/mol.[53] In some of the previous studies of transition metal complexes, the lack of reliable experimental results and the uncertainty of the calculated CASPT2 reference calculations tempered the reliability of the conclusions. Other factors also come into play in transition metal complexes, for example, multi-center delocalization, ionic–covalent resonance, and the noncovalent interaction between ligands and between metal centers and ligands. In contrast, in atoms with reliable experimental excitation energies, we can study the ability of approximate density functionals to balance exchange and correlation for the calculation of spin splittings with a minimum of additional considerations. For this reason we devote our attention in this study to a systematic exploration of p-block atoms, where it is easier to avoid multi-determinantal character than it is for transition metal atoms. Note, however, that the spin splittings in atoms have some characteristics that are quite different from spin splittings at weakly coupled centers, such as those best treated by the Heisenberg–Dirac–van Vleck model, so eventually the results for the different kinds of systems need to be understood in a more comprehensive framework.

Our work in this article is presented in the following order: Sec. II discusses the functionals we included in the present study; Sec. III describes the multiplicity-changing excitation energy database that we used to test the approximate functionals; the computational details are given in Sec. IV; Sec. V discusses basis set convergence; Secs. VI and VII present the results, including discussion; Sec. VIII presents a reduced-size representative database that may be useful in future work; and Sec. IX concludes the paper.

II. FUNCTIONALS STUDIED

Most DFT calculations are done with the Kohn–Sham formalism[2] and need to approximate the unknown xc functional. The different ways to approximate the unknown xc functional are usually classified according to the ingredients in the approximate functionals. The simplest functionals depend on only spin densities (i.e., the densities of spin-up and spin-down electrons), and they are called local spin density approximations (LSDAs). When the reduced gradients of spin densities are also introduced into the functional form, the resulting functionals are called generalized gradient approximations (GGAs). The functionals are called meta-GGAs when they utilize the spin densities, the reduced gradients of spin densities, and the spin-labeled kinetic energy densities (or the Laplacians of spin densities, but no functionals involving Laplacians are considered here). The functionals mentioned so far are all local in the sense that their xc potential at a point in the space only depends on the spin densities, reduced gradients, or spin-labeled kinetic energy densities at that point. In contrast, the Hartree–Fock exchange potential at one point depends on integrals over the Kohn–Sham orbitals in the whole space, so it is nonlocal. Replacing a fixed percentage X of local exchange by nonlocal Hartree–Fock exchange in GGA functionals leads to functionals that are called global hybrid GGA functionals. Global hybrid meta-GGA functionals are obtained by introducing a fixed percentage of Hartree–Fock exchange into meta-GGAs. In some functionals, an empirical molecular mechanics term is added to the DFT energy to account for damped dispersion-like interactions. This kind of functional is called a DFT-D or "-D" functional; if the MM term is added to a GGA, it may be labeled GGA-D. Range-separated hybrid functionals are defined by partitioning the Coulomb operator into a long-range and a short-range part and treating one of them by local exchange and the other by Hartree-Fock exchange.

In the ΔSCF calculations, we included three LSDAs, 11 GGAs, 16 global hybrid GGAs, seven range-separated hybrid GGAs, one range-separated hybrid GGA-D functional, three meta-GGAs, and 15 global hybrid meta-GGAs. The functionals that we tested are listed in Table I, with references for each of them.[44,59–62,71–109] Of the 56 xc functionals, 20 of them are included because of their good performance in a recent study[110] of density functionals against a database that contains various bond energies and barrier heights relevant to catalysis. These functionals are identified by a number in the last column of Table I; this number is their ranking in terms of averaged error for catalytic energies in that study. We will discuss the reason to include other functionals in the present study in the rest of this section.

LSDAs have generally good performance for predicting equilibrium geometries, and they have less error due to static correlation than many popular functionals, but they are not usually the best functionals for actual applications, due to poor energetic predictions. The three LSDA functionals are included in order to evaluate the performance of the simplest xc approximations for multiplicity-changing excitations. Also, they serve as a good reference to see the improvement of other approximations by including more ingredients and using more flexible functional forms.

Hartree–Fock (HF) theory is included, since, although not actually a density functional method, it can be seen as a density functional with $X = 100$ and no components other than Hartree-Fock exchange in the approximation to the xc functional. The HF approximation and the other two exchange-only approximations, B88 exchange[75] and OptX exchange,[59] provide references to study the effect of correlation for the multiplicity-changing excitations by comparing their predictions to those of HFLYP, HFPW91, BLYP, BPW91, OLYP, and OPBE. Among the latter, BLYP and BPW91 are two GGA functionals that have been widely used in both chemistry and physics. As mentioned in Sec. I, the OLYP and OPBE functionals, although not good general-purpose functionals, have excellent performance for the high-spin/low-spin energy splitting in some previous studies of iron complexes.[50–52,54] We note the PW91 and PBE correlation are very similar so BPBE would be similar to BPW91, OPW91 would be similar to OPBE, and so forth.

The B3LYP* functional is a reparameterization by Reiher and coworkers,[44] specifically for spin-state energetics of transition metal complexes, of the widely used B3LYP functional. The only change is that the percentage of Hartree–Fock exchange, X, is reduced from 20 to 15. Because the B3LYP*

TABLE I. Tested density functionals.

Type	Name	References	Rank[a]
LSDA	SPL	71, 72	
	SPWL	71, 73	
	SVWN	71, 74	
GGA	BLYP	61, 75	
	BPW91	75, 76	
	B88[b]	75	
	MOHLYP	77	17
	mPWLYP	61, 78	
	OLYP	59, 61	
	OPBE	59, 60	
	OptX[b]	59	
	PBE	60	
	PW91	76	
	RPBE	79	20
Global hybrid GGA	B3LYP	80	12
	B3LYP*	44	
	B3LYP54	present	
	B3LYP60	present	
	B3PW91	81	10
	B3V5LYP	82	14
	B97-3	83	6
	B98	84	7
	HFLYP[c]	61	
	HFPW91[c]	76	
	MPW1K	85	
	MPW1PW91	78	
	MPW3LYP	86	
	MPWLYP1M	77	18
	O3LYP	87	
	PBE1[d]	88	11
Range-separated hybrid GGA	CAM-B3LYP	89	
	HSE	90, 91	13
	LC-MPWLYP[e]	92	
	LC-OLYP[e]	92	
	LC-OPBE[e]	92	
	LC-ωPBE	93	16
	ωB97X	94	
Range-separated hybrid GGA-D	ωB97X-D	95	5
Meta-GGA	M06-L	96	3
	TPSS	97	
	VS98[f]	98	8
Global hybrid meta-GGA	BMK	99	15
	M05	100	2
	M05-2X	101	
	M06	102	1
	M06-2X	102	
	M06-HF	103	
	M08-HX	104	
	M08-SO	104	
	MPW1KCIS	78, 105, 106	
	MPWKCIS1K	78, 105, 106	
	PW6B95	107	
	PWB6K	107	
	TPSSh	62	19
	TPSS1KCIS	97, 105, 108	9
	τHCTHhyb	109	4

[a]Ranking on catalytic energies database of Ref. 110.
[b]Density functional exchange with no correlation.
[c]Hartree–Fock (HF) exchange with density functional correlation.
[d]Also called PBE0, PBE1PBE, or PBEh.
[e]Obtained by applying Hirao's long-range correction[92] to the indicated GGA.
[f]Also called VSXC.

functional yields more accurate estimations than B3LYP for the high-spin/low-spin energy splittings for some iron complexes, it is quite interesting to compare its performance to that of B3LYP for the multiplicity-changing excitation energies of p-block elements, and so we included it in the present study. In the present article we will also consider other B3LYP modifications obtained by raising X. In particular we consider two new functionals called B3LYP54 and B3LYP60 in which X is 54 and 60, respectively. These two functionals are inspired by previous results for singlet–triplet splittings,[19] where $X = 50$ was found to be optimal. We also consider B3LYP0, where X is 0 but for technical reasons is set to 0.001.

The MPW3LYP functional was constructed in the same spirit as B3LYP; however, the B88 exchange is replaced by the mPW exchange, and the percentage of Hartree–Fock exchange is notably raised to 21.8. Another closely related functional is MPWLYP1M, which contains only 5% Hartree–Fock exchange, and is designed for transition metal systems.

The range-separated hybrid functionals involve partitioning the two-electron Coulomb operator, $1/r_{12}$, into short-range and long-range parts, as first proposed by Savin.[111] The original approach to range separation was to treat the short-range interactions by density functional exchange and the long-range interactions by Hartree–Fock exchange. The functionals developed with this approach are called long-range-corrected functionals. Since they have 100% Hartree–Fock exchange in the long-range limit, they have the correct asymptotic behavior and are supposed to yield better performance for Rydberg and charge-transfer excitations.[112] An alternative approach is to treat the short-range exchange by Hartree–Fock exchange and the long-range exchange by local density functional exchange. Functionals developed with this approach are called screened Coulomb hybrid functionals. The HSE functional is constructed with this approach, and it yields good performance for solid-state calculations.[90]

When an analytic expression of the exchange hole is available, the short-range density functional exchange can be derived without difficulty. For example, the short-range Slater exchange was derived more than one decade ago.[113] In the ωB97X and ωB97X-D functionals, the short-range B97 exchange is obtained by using the short-range Slater exchange multiplied by the gradient enhancement factor of the B97 exchange. In the LC-ωPBE functional, the short-range PBE exchange was derived by using the model PBE exchange hole.[114] In 2001, Hirao and coworkers introduced a general approach to obtain the short-range density functional exchange from conventional GGAs.[92] The LC-MPWLYP, LC-OLYP, and LC-OPBE functionals tested here are obtained with Hirao's approach for the short-range exchange.

The Coulomb-attenuating method based on B3LYP (CAM-B3LYP) was also constructed with the range-separation approach. The CAM-B3LYP exchange functional has 19% Hartree–Fock exchange plus 81% B88 exchange at short range, and 65% Hartree–Fock exchange plus 35% B88 exchange at long range. A recent TDDFT study has shown excellent performance of CAM-B3LYP for valence, Rydberg, and charge-transfer excitations.[115]

PBE, as well as its early version PW91, and the related meta-GGA functional TPSS were constructed with the philosophy of determining parameters by forcing the functionals

to satisfy physical constraints selectively chosen on the basis of theoretical availability and previous experience. Global hybrid versions, PBE1 and TPSSh, are obtained by introducing 25% and 10% Hartree–Fock exchange in the PBE and TPSS functionals. Note that PBE1 is sometimes called PBE0, PBE1PBE, or PBEh (it should not be confused with the PBE-hole functional, although both have sometimes been called PBEh).

The PW6B95 (6-parameter functional based on Perdew-Wang '91 exchange and Becke '95 correlation) and PWB6K (6-parameter functional for kinetics based on Perdew-Wang '91 exchange and Becke '95 correlation) are hybrid meta-GGA functionals optimized against small binding-energy and barrier-height databases. The PW6B95 functional was singled out for good performance in a recent study[116] of a general main-group database for thermochemistry, kinetics, and noncovalent interactions.

The Minnesota M05-class, M06-class, and M08-class functionals were developed with the philosophy of optimizing functionals for general applications by using carefully designed but flexible functional forms and very diverse training sets. They have shown excellent performance for many interesting chemical systems, as shown in three recent reviews.[117–119] M06-L is among the most accurate functionals for transition metals, and, along with MOHLYP, it is the best local functional for barrier heights. M05 and M06 are general functionals for transition metals, main group thermochemistry, and barrier heights. M06-HF represents an attempt to improve the valence, Rydberg, and charge-transfer excitations without much sacrifice to the ground-state accuracy. M05-2X and M06-2X perform well for main-group thermochemistry, barrier heights, and noncovalent interactions. M08-HX is an attempt to improve the performance of M05-2X and M06-2X with a more flexible functional form, and M08-SO is a version of M08-HX designed to be correct through second order for the deviation of exchange and correlation from the uniform density limit. A recent TDDFT study[120] showed that M06-2X and M08-HX perform as well as, and in some cases better than CAM-B3LYP for charge transfer excitations with intermediate spatial overlap, which is encouraging since their mean unsigned errors are more than a factor of four smaller than CAM-B3LYP's for bond energies and noncovalent binding energies and more than a factor of two smaller for barrier heights.[120]

High-exchange global hybrid functionals were not included in the catalytic energies study[110] because the catalytic energies database includes transition metals, and we do not recommend current high-exchange density functionals for systems containing transition metals. The high-exchange global hybrid functionals included in the present study are (with X indicated in parentheses): HFLYP (100), HFPW91 (100), BMK (42), M05-2X (56), M06-2X (54), M06-HF (100), M08-HX (52.23), M08-SO (56.79), and PWB6K (46).

For LS-TDDFT calculations, we only tested a few of the functionals employed for the ΔSCF calculations. Two exchange-only approximations, HF and B88, and ten representative functionals, namely, SVWN, PBE, B3LYP, B3LYP54, B3LYP60, M06-L, M06, LC-ωPBE, HSE, and ωB97X-D, plus the three best functionals in the ΔSCF study, were included for the LS-TDDFT study. For SF-TDDFT calculations, we tested B3LYP0, B3LYP*, B3LYP, B3LYP54, B3LYP60, M06, M06-2X, O3LYP, PWB6K, ωB97X, ωB97X-D, and HF.

III. DATABASES

Among all the elements of the 2p, 3p, and 4p blocks of the periodic table, we selected all neutral atoms and monocations with ground states and spin-excited states that can both be well represented by a single Slater determinant and for which the ground state is the low-spin one. This leads to a database containing B, B^+, C^+, F, Ne, Ne^+, Al, Al^+, Si^+, Cl, Ar, Ga, Ga^+, Ge^+, Br, Kr, and Kr^+.

Scalar relativistic effects were taken into account in the present paper, but not spin-orbit coupling, which is a vector relativistic effect. Therefore we removed spin-orbit effects from the experimental data to which we compare. Because spin-orbit coupling is weak for atoms no heavier than Kr, it is sufficient to remove it to first order. The spin-orbit operator is traceless; therefore it can be removed from the experimental excitation energies (which were taken from data published by Moore[121]) by a simple degeneracy-weighted average:

$$\overline{E}(^{2S+1}L) = \frac{\sum_{J=|L-S|}^{L+S}(2J+1)E(^{2S+1}L_J)}{\sum_{J=|L-S|}^{L+S}(2J+1)}. \quad (1)$$

The experimental values we used to test the performance of density functionals are all spin-orbit-free excitation energies obtained in this way, and they are listed in Tables V and VI.

In the excitations of B, B^+, C^+, Al, Al^+, Si^+, Ga, Ga^+, and Ge^+, an electron is excited from an ns orbital to an np orbital. This kind of excitation is called a valence excitation. We compiled the excitation energies of these nine cases to form a database with nine p-block multiplicity-changing valence excitation energies that may be labeled pB-MC-VEE9. In the excitations of F, Ne, Ne^+, Cl, Ar, Br, Kr, and Kr^+, an electron is excited from an np orbital to an $(n+1)s$ orbital. This kind of excitation is called a Rydberg excitation. We compiled the excitation energies of these eight cases to form a database with 8 p-block multiplicity-changing Rydberg excitation energies (pB-MC-REE8). The pB-MC-VEE9 and pB-MC-REE8 databases are combined into a merged database, the 17 p-block multiplicity-changing valence and Rydberg excitation energies (pB-MC-VREE17) database. It can be used to evaluate the overall performance of a functional for atomic valence and Rydberg excitations. In the rest of the article we will abbreviate the pB-MC-VEE9, pB-MC-REE8, and pB-MC-VREE17 databases as V9, R8, and VR17, respectively. For future testing where smaller databases may be desirable, two representative subsets containing four excitation energies each, are compiled and are called the V4 and R4 databases, as discussed in Sec. VIII.

IV. COMPUTATIONAL DETAILS

The ΔSCF and LS-TDDFT calculations were performed with locally modified versions of GAUSSIAN03 (Ref. 122) and GAUSSIAN09.[123] The spin-unrestricted formalism was used for all the atoms and cations. In order to obtain the lowest-energy solutions to the Kohn-Sham equations, we allowed different orbitals for different spins, and we did not require the orbitals to be symmetry orbitals. However, the optimized orbitals turn out to be symmetry orbital in our cases, which means that they are eigenfunctions of the square of the orbital angular momentum. We did not require all p orbitals to have the same radial factor for states with both singly and doubly occupied p orbitals (likewise, we did not use equivalence restrictions). We always did stability tests[124,125] to confirm that we had obtained the lowest-energy state for each multiplicity. The DFT calculations were carried out with a pruned grid having 99 radial shells and 590 angular points for each shell (this is called the ultrafine grid in the GAUSSIAN software).

For valence excitations, the cc-pVTZ and cc-pVQZ basis sets[126–128] were used to study basis set convergence. Another valence quadruple zeta basis set,[129] namely, def2-QZVP, was used to confirm that the basis set limit was obtained and that the results are not sensitive to the chosen basis sets. For Rydberg excitations, the cc-pVTZ, cc-pVQZ, and cc-pV5Z basis sets[126–128] were used first. Then the effect of diffuse functions was studied by adding diffuse functions to the cc-pVQZ basis set. By adding a diffuse function to each angular symmetry in the cc-pVQZ basis set, the augmented polarized valence correlation consistent basis set is obtained, which is usually denoted as aug-cc-pVQZ. In 1993, Woon and Dunning proposed multiply augmented basis sets by adding even-tempered sets of diffuse functions to the correlation consistent basis sets of Dunning and co-workers.[130] With multiply augmented basis sets, they were able to obtained converged results for the electrical properties of the rare gas atoms. Following the same idea, we generated doubly and triply augmented basis sets for F, Ne, Cl, Ar, Br, and Kr; when two and three diffuse functions of each symmetry are added to the cc-pVQZ basis set, the resulting basis sets are called doubly and triply augmented polarized valence correlation consistent quadruple zeta basis sets, denoted as d-aug-cc-pVQZ and t-aug-cc-pVQZ.[130] Following the procedure used for the minimally augmented Karlsruhe basis sets (ma-SVP, ma-TZVP, and ma-QZVP),[131] which use geometric series of diffuse exponential parameters differing by factors of three to obtain the s and p diffuse functions for all elements except H, a minimally doubly augmented quadruple zeta basis, mda-QZVP, was obtained by dividing the most diffuse exponential parameter by three and nine to obtained the first and second sets of s and p diffuse functions.

The scalar relativistic effect was included in the ΔSCF and LS-TDDFT calculations by using the Douglas-Kroll-Hess (DKH) second-order scalar relativistic Hamiltonian.[132–134] In the relativistic calculations, the cc-pVQZ-DK and d-aug-cc-pVQZ-DK basis sets were used for valence and Rydberg excitations, respectively; the cc-pVQZ-DK basis set is a recontraction of cc-pVQZ basis set for DKH calculations by de Jong *et al.*,[135] and the d-aug-cc-pVQZ-DK basis set was obtained by adding the diffuse functions of the d-aug-cc-pVQZ basis to the cc-pVQZ-DK basis set.

High level *ab initio* CCSD(T)[136] calculations, with the DKH Hamiltonian to account for the scalar relativistic effect, were performed with GAUSSIAN09. In these calculations, very extensive cc-pVnZ-DK and d-aug-cc-pVnZ-DK (n = Q and 5) basis sets were used for V9 and R8 database, respectively. These are unrestricted coupled cluster calculations based on unrestricted Hartree-Fock orbitals without requiring symmetry orbitals.

The SF-TDDFT calculations were performed with the *Q-Chem* program.[137] The formulation of SF-TDDFT implemented in *Q-Chem* is the collinear one,[19] i.e., the xc potential only depends on the α and β spin densities, and it uses the Tamm–Dancoff[34,138,139] approximation (whereas the low-spin TDDFT calculations do not involve this additional approximation). Within the collinear TDDFT approach, only the Hartree-Fock exchange part of the functional contributes to the SF coupling.[19] Therefore, only hybrid density functionals can be employed in this formulation. For the reference states (a triplet state with $M_S = 1$ for singlet–triplet transitions and a quartet state with $M_S = 3/2$ for doublet–quartet transitions) the calculations were carried out with a grid composed of 120 radial points and 302 Lebedev angular points. For valence excitations we employed the cc-pVQZ basis set and for Rydberg excitations we used the aug-cc-pVQZ and d-aug-cc-pVQZ basis sets. In the latter, diffuse g-functions were removed due to computational limitations. Scalar relativistic effects calculated at the ΔSCF level (as discussed further in Sec. VI) were added to the SF-TDDFT results for a better comparison with experiment.

An important computational consideration in SF-TDDFT is which state is used to represent the high-spin state. Consider the case of a triplet reference state. One generates both the singlet states and the $M_S = 0$ components of the triplet states by single-electron transitions from this state. In principle the $M_S = 0$ component of the triplet would have the same energy as the reference state (which has $M_S = 1$), but actually they may differ by up to several eVs. We follow the usual procedure of calculating the singlet–triplet spin splitting from the $M_S = 0$ component because this is a more consistent way to compare the states. Similarly we calculate doublet–quartet spin splittings by using the $M_S = 1/2$ component of the quartet, not by using the $M_S = 3/2$ reference state.

V. BASIS SET CONVERGENCE STUDIES

Ten different theoretical levels were used to test the basis set convergence of the ΔSCF calculations for the valence and Rydberg excitations. The ten levels include two exchange-only approximations, namely, HF and B88, and eight exchange-correlation functionals, SVWN, PBE, B3LYP, LC-ωPBE, HSE, ωB97X-D, M06-L, and M06. All convergence studies in this section are nonrelativistic.

As shown in Table II, the calculated valence excitation energies with the cc-pVTZ and cc-pVQZ basis sets agree quite well, with most of them differing by only a few tenths

TABLE II. The basis set effect on the nonrelativistic ΔSCF valence excitation energies of the V9 database (kcal/mol).

Functional	B^+	B	C^+	Al^+	Al	Si^+	Ga^+	Ga	Ge^+	MSE	MUE
					cc-pVTZ						
HF	72.58	50.68	84.32	81.87	55.51	89.78	100.69	71.00	104.12	− 34.65	34.65
B88	73.74	53.14	89.11	89.50	62.66	99.42	125.76	94.96	132.31	− 22.42	22.42
SVWN	93.43	74.35	111.63	108.08	83.65	122.45	143.58	115.50	154.05	− 1.74	6.30
PBE	91.81	75.74	114.01	104.29	82.27	120.78	137.02	110.42	148.88	− 4.13	4.86
B3LYP	94.88	83.28	122.44	108.49	87.84	126.60	138.54	113.85	151.95	0.61	3.36
LC-ωPBE	90.08	73.14	111.43	96.92	75.43	113.28	123.25	97.13	136.05	− 11.74	11.74
HSE	90.58	74.45	111.74	101.62	79.73	117.44	130.87	104.66	142.04	− 7.69	7.69
ωB97X-D	87.53	71.55	106.37	99.64	77.63	114.43	138.70	114.52	150.83	− 6.80	9.01
M06-L	90.32	77.22	114.19	106.05	82.75	121.23	142.01	117.12	153.06	− 2.05	6.07
M06	96.52	82.04	119.77	110.40	88.05	128.31	152.23	126.88	164.86	5.19	8.24
					cc-pVQZ						
HF	72.28	50.52	83.97	81.19	55.11	89.31	99.75	70.45	103.94	− 35.10	35.10
B88	73.48	53.01	88.88	89.11	62.60	99.05	125.83	95.57	132.20	− 22.52	22.52
SVWN	93.35	74.21	111.47	107.81	83.60	122.22	143.52	115.69	154.02	− 1.83	6.35
PBE	91.60	75.58	113.77	103.88	82.15	120.46	137.03	110.79	148.74	− 4.26	5.04
B3LYP	94.64	83.10	122.17	108.05	87.64	126.26	138.29	113.93	151.88	0.40	3.26
LC-ωPBE	89.91	73.03	111.21	96.41	75.10	112.97	123.30	97.28	135.91	− 11.92	11.92
HSE	90.38	74.31	111.50	101.14	79.48	117.06	130.50	104.63	141.88	− 7.94	7.94
ωB97X-D	87.48	71.51	106.45	99.42	77.60	114.02	138.28	114.43	150.61	− 6.95	9.01
M06-L	90.22	76.77	113.94	105.39	81.93	120.41	141.27	116.44	153.37	− 2.52	6.29
M06	96.24	81.51	119.20	109.74	87.79	127.67	150.99	126.11	164.20	4.57	7.92
					def2-QZVP						
HF	72.21	50.47	83.87	81.07	55.04	89.23	99.76	70.44	103.93	− 35.15	35.15
B88	73.39	52.97	88.74	89.10	62.67	99.14	126.08	95.81	132.38	− 22.46	22.46
SVWN	93.26	74.17	111.35	107.68	83.53	122.20	143.66	115.87	154.09	− 1.84	6.40
PBE	91.54	75.50	113.62	103.74	82.06	120.36	137.14	110.85	148.77	− 4.31	5.11
B3LYP	94.54	83.03	122.03	107.92	87.57	126.19	138.33	113.95	151.84	0.33	3.25
LC-ωPBE	89.83	72.92	111.05	96.30	75.04	112.89	123.45	97.37	135.98	− 11.95	11.95
HSE	90.28	74.21	111.33	101.05	79.44	117.01	130.64	104.72	141.95	− 7.97	7.97
ωB97X-D	87.33	71.38	106.17	99.53	77.75	114.29	138.62	114.73	150.91	− 6.85	9.12
M06-L	89.91	76.92	113.99	105.72	82.16	120.68	141.21	116.36	153.32	− 2.46	6.19
M06	95.85	81.34	118.93	110.23	88.07	128.12	151.52	126.85	164.74	4.81	8.35

of a kcal/mol. The agreement between the cc-pVTZ and cc-pVQZ results suggests that the complete basis limit is reached to a good approximation with the cc-pVQZ basis set. The excitation energies calculated by def2-QZVP agree quite well with those calculated by cc-pVQZ, further confirming that the cc-pVQZ basis set is large enough for the valence excitations of the V9 database.

Basis set effects on TDDFT calculations of Rydberg excitations have been studied recently by Ciofini and Adamo, and the importance of diffuse function for the correct description of Rydberg excitations has been highlighted.[140] Even Dunning's augmented correlation consistent basis sets, aug-cc-pVnZ (n = D, T, Q, or 5), are not enough to yield reliable results for Rydberg excitations.[141] Previous studies on Rydberg excitations have shown that doubly(or triply) augmented basis sets are able to yield reasonable results for Rydberg excitations.[141–143] Similar trend is observed in our study, as shown in Table III. The calculated Rydberg excitation energies decrease on the order of 10 kcal/mol when we further augment the aug-cc-pVQZ to d-aug-cc-pVQZ basis sets. And MUEs of most tested functionals also decrease. It is interesting to point out that the MUEs of the exchange-only approximations, HF and B88, increase when the d-aug-cc-pVQZ basis set is used. This indicates that the better performance of HF and B88 with aug-cc-pVQZ is a result of error cancellation between lack of correlation and basis set incompleteness.

Further augmentation with diffuse functions has little effect on the calculated excitation energies; in particular, one can see that the t-aug-cc-pVQZ and d-aug-cc-pVQZ give nearly identical results, with difference of only few hundredths of a kcal/mol. As described in Sec. IV, we also generated minimally doubly augmented basis sets, mda-QZVP, for F, Ne, Cl, Ar, Br, and Kr. Results of the calculations of the Rydberg excitation energies with this new basis set are listed in Table III. For most of the methods, the mda-QZVP results agree with those obtained from d-aug-cc-pVQZ. Based on the agreement of d-aug-cc-pVQZ and t-aug-cc-pVQZ, as well as the agreement of d-aug-cc-pVQZ and mda-QZVP, we are quite confident that the DFT complete basis limit of the Rydberg excitation is reasonably well obtained when d-aug-cc-pVQZ is used.

VI. SCALAR RELATIVISTIC EFFECTS

Both non-relativistic (NR) and DKH scalar relativistic ΔSCF calculations were performed for the valence and

TABLE III. The basis set effect of diffuse functions on the nonrelativistic ΔSCF Rydberg excitation energies of the R8 database.

Functional	F	Ne	Ne^+	Cl	Ar	Br	Kr	Kr^+	MSE	MUE
					cc-pVQZ					
HF	496.85	646.42	804.40	303.79	391.42	248.37	307.64	343.20	128.43	128.43
B88	489.91	636.65	791.79	287.17	394.99	232.35	288.52	337.42	118.01	118.01
SVWN	519.83	670.02	825.69	312.99	397.28	261.33	315.45	362.08	143.75	143.75
PBE	509.75	654.70	814.55	305.53	390.91	250.38	306.11	351.73	133.62	133.62
B3LYP	514.87	658.89	820.37	311.81	395.39	257.14	311.96	358.41	139.27	139.27
LC-ωPBE	523.13	667.39	828.11	319.75	391.33	273.06	320.71	357.21	145.75	145.75
HSE	511.14	656.71	817.89	309.41	402.55	254.62	310.87	354.12	137.83	137.83
ωB97X-D	520.04	666.52	828.24	320.28	391.76	264.46	319.97	361.03	144.70	144.70
M06-L	614.09	787.48	914.62	371.06	384.66	312.41	370.92	386.92	203.43	203.43
M06	518.79	668.32	829.78	312.56	384.93	254.32	310.72	358.76	140.44	140.44
					aug-cc-pVQZ					
HF	277.84	375.34	598.60	195.01	259.78	172.65	226.11	311.90	− 12.18	12.18
B88	289.42	386.55	603.85	189.92	252.88	164.98	215.91	299.53	− 13.96	14.45
SVWN	320.49	420.81	637.88	215.64	278.85	190.44	240.79	327.07	14.66	14.66
PBE	311.10	406.99	627.75	210.22	272.59	184.31	234.67	320.45	6.68	7.04
B3LYP	312.70	406.84	630.17	212.89	273.90	187.97	236.94	324.54	8.91	8.91
LC-ωPBE	300.49	387.08	634.12	211.39	270.52	188.25	236.62	332.03	5.73	5.73
HSE	308.45	404.36	627.17	211.31	274.34	186.53	237.30	324.02	7.35	7.35
ωB97X-D	317.13	414.27	639.16	220.51	283.43	194.61	244.37	333.08	16.49	16.49
M06-L	319.46	415.01	644.34	224.66	291.78	195.41	245.74	336.97	19.84	19.84
M06	319.39	419.13	644.26	217.40	283.57	189.66	239.93	328.45	15.89	15.89
					d-aug-cc-pVQZ					
HF	256.66	343.96	595.23	185.58	246.27	166.10	217.01	311.51	− 24.05	24.05
B88	270.99	358.65	601.06	182.50	241.89	160.17	208.98	299.29	− 23.89	23.89
SVWN	304.56	396.14	635.70	210.27	270.55	187.30	236.06	327.00	6.61	6.61
PBE	293.93	380.82	625.16	203.60	262.80	180.15	228.70	320.26	− 2.41	2.67
B3LYP	295.59	381.11	627.71	206.25	264.29	183.72	231.03	324.38	− 0.07	2.38
LC-ωPBE	300.49	387.10	634.16	211.39	270.52	188.26	236.63	332.03	5.74	5.74
HSE	290.83	377.56	624.57	204.54	264.29	182.26	231.16	323.83	− 1.95	2.78
ωB97X-D	298.22	386.00	636.29	212.53	272.07	189.21	237.00	332.81	6.18	6.18
M06-L	303.48	389.84	642.48	218.95	282.79	192.04	240.51	332.20	10.95	10.95
M06	302.21	392.78	641.82	210.97	274.13	185.30	233.84	328.25	6.83	6.83
					t-aug-cc-pVQZ					
HF	256.64	343.85	595.17	185.57	246.25	166.10	217.00	311.51	− 24.07	24.07
B88	270.97	358.55	601.02	182.50	241.88	160.17	208.97	299.29	− 23.92	23.92
SVWN	304.56	396.12	635.67	210.26	270.54	187.29	236.04	327.00	6.60	6.60
PBE	293.92	380.76	625.13	203.60	262.80	180.15	228.69	320.26	− 2.42	2.68
B3LYP	295.58	381.06	627.68	206.25	264.29	183.72	231.02	324.38	− 0.09	2.38
LC-ωPBE	300.49	387.08	634.12	211.39	270.52	188.25	236.62	332.03	5.73	5.73
HSE	290.82	377.51	624.53	204.54	264.29	182.25	231.16	323.83	− 1.97	2.79
ωB97X-D	298.20	385.89	636.25	212.52	272.06	189.21	236.99	332.81	6.16	6.16
M06-L	303.44	389.84	642.48	218.85	282.72	191.94	240.40	332.13	10.89	9.51
M06	302.20	392.70	641.81	210.97	274.13	185.29	233.82	328.25	6.81	6.26
					mda-QZVP					
HF	256.71	344.06	595.51	185.69	246.35	166.31	217.25	311.88	− 23.87	22.84
B88	270.96	358.60	601.05	182.64	242.01	160.65	209.46	300.20	− 23.64	21.20
SVWN	304.56	396.07	635.66	210.41	270.68	187.67	236.42	327.73	6.82	6.32
PBE	293.93	380.82	625.16	203.60	262.80	180.15	228.70	320.26	− 2.41	3.50
B3LYP	295.53	381.01	627.75	206.32	264.35	184.01	231.32	324.92	0.07	2.24
LC-ωPBE	300.40	386.97	634.12	211.46	270.58	188.60	236.97	332.69	5.89	5.97
HSE	290.80	377.51	624.69	204.64	264.39	182.58	231.51	324.53	− 1.75	2.83
ωB97X-D	298.22	386.00	636.29	212.53	272.07	189.21	237.00	332.81	6.18	6.18
M06-L	304.04	391.09	641.68	219.39	283.19	192.25	240.92	337.54	11.93	11.93
M06	302.24	393.31	641.13	210.93	274.01	185.56	234.26	328.51	6.91	6.91

TABLE IV. Scalar relativistic effects on the ΔSCF excitation energies of the VR17 database.[a]

V9			R8		
B^+	$2s^2 \rightarrow 2s^1 2p^1$	0.16	F	$2s^2 2p^5 \rightarrow 2s^2 2p^4 3s^1$	−0.39
B	$2s^2 2p^1 \rightarrow 2s^1 2p^2$	0.12	Ne^+	$2s^2 2p^5 \rightarrow 2s^2 2p^4 3s^1$	−0.70
C^+	$2s^2 2p^1 \rightarrow 2s^1 2p^2$	0.35	Ne	$2s^2 2p^6 \rightarrow 2s^2 2p^5 3s^1$	−0.52
Al^+	$3s^2 \rightarrow 3s^1 3p^1$	0.84	Cl	$3s^2 3p^5 \rightarrow 3s^2 3p^4 4s^1$	−0.66
Al	$3s^2 3p^1 \rightarrow 3s^1 3p^2$	0.71	Ar	$3s^2 3p^6 \rightarrow 3s^2 3p^5 4s^1$	−0.76
Si^+	$3s^2 3p^1 \rightarrow 3s^1 3p^2$	1.37			
Ga^+	$4s^2 \rightarrow 4s^1 4p^1$	6.99	Br	$4s^2 4p^5 \rightarrow 4s^2 4p^4 5s^1$	−2.03
Ga	$4s^2 4p^1 \rightarrow 4s^1 4p^2$	6.17	Kr^+	$4s^2 4p^5 \rightarrow 4s^2 4p^4 5s^1$	−2.86
Ge^+	$4s^2 4p^1 \rightarrow 4s^1 4p^2$	9.03	Kr	$4s^2 4p^6 \rightarrow 4s^2 4p^5 5s^1$	−2.01

[a]The scalar relativistic corrections are evaluated by taking the difference of excitation energies calculated by DKH calculation with cc-pVQZ-DK (or d-aug-cc-pVQZ-DK) and non-relativistic calculations with cc-pVQZ (or d-aug-cc-pVQZ) averaged over HF and 56 tested functionals.

Rydberg excitation energies in the VR17 database. Table IV lists the electron configurations and the calculated scalar relativistic effects for all excitations. The estimated scalar relativistic corrections were obtained by taking the average of the DKH and NR differences over the ΔSCF results for all tested methods.

The scalar relativistic effect stabilizes *s* electrons relative to *p* electrons. This is clearly shown in Table IV. For the valence excitations in the V9 database, where the excitation involves a transition from an *ns* orbital to an *np* orbital, the scalar relativistic effects are positive, which means the scalar relativistic effect increases the excitation energies. On the other hand, in the R8 database, where the excitation involves a transition from an *np* orbital to an $(n + 1)s$ orbital, the scalar relativistic effects are negative.

The scalar relativistic effect of the cations is larger than that of their neutral counterparts, which is understandable since the electrons are closer to the nucleus in the cations. The scalar relativistic correction is quite small for B, B^+, and C^+, on the order of a few tenths of kcal/mol. For F, Ne^+, Ne, Al, Al^+, Si^+, Cl, and Ar, the scalar relativistic correction is still quite small, usually smaller than 1 kcal/mol, but not negligible for quantitative results. For the valence excitations of 4p elements (Ga and Ge), the scalar relativistic effect becomes quite large, 6–9 kcal/mol, so the scalar relativistic effect should always be taken into account for multiplicity-changing valence excitations for the 4p elements. The scalar relativistic corrections to the Rydberg excitations are somewhat smaller than those to valence excitations. However, they are still 2–3 kcal/mol for Br, Kr^+ and Kr and should always be taken into account for quantitative results. The DKH Hamiltonian was used to account for the scalar relativistic effect for ΔSCF calculations throughout the paper, except for Tables II and III that report nonrelativistic results, as indicated in the table heading.

VII. MULTIPLICITY-CHANGING EXCITATION ENERGIES

A. ΔSCF

In Tables V and VI, the spin-orbit-free (see Eq. (1)) experimental excitation energies are listed in the second row. The DKH-calculated valence excitation energies of various functionals with the cc-pVQZ-DK basis set, as well as the mean signed errors (MSEs) and mean unsigned errors (MUEs) are listed in Table V. The DKH-calculated Rydberg excitation energies of various functionals with d-aug-cc-pVQZ-DK basis set and the corresponding MSEs and MUEs are tabulated in Table VI. The MUE is used to evaluate the performance of a density functional, and the MSE will show whether there is a systematic trend to overestimate (positive MSE) or underestimate (negative MSE) the calculated low-spin-to-high-spin excitation energies. The MUEs of CCSD(T) with cc-pV5Z-DK (for the V9 database) and d-aug-cc-pV5Z-DK (for the R8 database) are 2.7 and 1.4 kcal/mol, respectively. The CCSD(T) calculated valence and Rydberg excitation energies are listed in the third row of Tables V and VI, for comparison to the performance of various density functionals.

1. Valence excitations

Due to the lack of correlation, the exchange-only approximations B88, OptX, and HF strongly underestimate the valence excitation energies, with MSEs of –20, –25, and –32 kcal/mol, respectively, which means that the exchange-only methods strongly favor the high-spin excited states. This is a well known trend for HF, which may be explained by recalling that the Fermi hole is included in Hartree–Fock exchange, but not the Coulomb hole. Our results show that the trend to stabilize the high-spin states is less dramatic for the B88 and OptX GGA exchange functionals than for Hartree–Fock exchange. By adding the Lee-Yang-Parr (LYP) correlation functional, the resulting MSEs of the BLYP, OLYP, and HFLYP functionals are much less negative, and the MUEs are much smaller. The MUEs of BLYP, OLYP, and HFLYP are 9, 4, and 6 kcal/mol, respectively. Similar trends can be observed when adding PW91 correlation to the HF and B88 exchange. However, the MSE of HFPW91 is still quite negative, –18 kcal/mol, and the MUE of HFPW91 is still quite large, 18 kcal/mol. This might be a result of the incompatibility of the HF exchange and the PW91 correlation. Note that although we do not show the combination of the OptX exchange with PW91 correlation, the PBE correlation in OPBE is very similar to the PW91 correlation.

The three LSDAs in Table V give MUEs of only 9 kcal/mol, which is surprising by considering the simplicity of those functionals and the fact that most of the more complicated functionals tested have MUEs larger than 6 kcal/mol.

It has sometimes been pointed out that standard local functionals (like LSDA, BLYP, etc.) systematically overstabilize low-spin states, while hybrid functionals (like B3LYP and PBE1) do better.[44,54] We do observe that some GGA functionals, such as BLYP and mPWLYP, tend to overstabilize the low-spin states, giving too high excitation energies. But there are also some GGA functionals, such as BPW91, OPBE, PBE, PW91, and RPBE, which on average favor high-spin states relative to low-spin states, giving negative MSEs. The BPW91, PBE, PW91, and RPBE functionals underestimate the excitation energies of the first and second row elements (B, C, Al, and Si) but overestimate the

TABLE V. The performance of relativistic CCSD(T) and ΔSCF calculations with various functionals for the valence excitations of the V9 database (kcal/mol).[a]

	B^+	B	C^+	Al^+	Al	Si^+	Ga^+	Ga	Ge^+		
Expt.[b]	106.78	82.35	122.92	107.27	82.98	126.00	138.05	108.69	147.34	MSE	MUE
CCSD(T)	107.40	82.83	123.18	104.23	79.99	119.14	134.99	105.60	143.32	− 2.41	2.71
Exchange only											
B88	73.63	53.13	89.23	89.94	63.32	100.43	133.21	102.24	141.75	− 19.50	19.50
HF	72.43	50.64	84.31	81.98	55.78	90.62	105.91	75.83	112.09	− 32.53	32.53
OptX	77.61	53.97	89.13	84.76	57.90	92.47	121.97	90.09	127.16	− 25.26	25.26
LSDA											
SPL	94.73	75.75	113.14	109.46	85.44	124.76	151.37	123.06	164.36	2.19	8.78
SPWL	94.24	75.74	113.25	108.98	85.23	124.52	150.47	122.22	163.43	1.74	8.48
SVWN	93.50	74.33	111.81	108.67	84.34	123.62	151.04	122.40	162.71	1.12	8.85
GGA											
BLYP	95.09	84.85	124.88	110.80	90.82	130.64	151.02	126.34	167.83	6.66	9.25
BPW91	88.95	73.12	110.66	100.71	78.99	117.21	141.58	114.35	154.39	− 4.71	8.32
MOHLYP	101.93	87.50	128.16	106.38	85.95	124.09	140.82	115.02	154.55	2.45	4.15
mPWLYP	96.43	86.27	126.61	112.82	92.79	132.95	152.26	127.60	169.47	8.31	10.61
OLYP	99.03	85.63	124.71	105.46	85.17	122.42	140.04	114.36	153.37	0.87	3.79
OPBE	92.89	73.82	110.26	95.11	73.23	108.71	129.51	101.44	138.96	− 10.94	10.94
PBE	91.76	75.71	114.12	104.71	82.87	121.83	144.35	117.26	158.09	− 1.30	6.99
PW91	91.61	75.80	113.98	104.77	82.90	121.80	144.26	117.04	157.84	− 1.37	6.94
RPBE	94.33	78.86	118.00	104.14	83.00	121.60	141.53	114.83	155.21	− 1.21	5.10
Hybrid GGA											
B3LYP	94.80	83.22	122.53	108.90	88.38	127.65	145.36	120.22	161.04	3.30	6.05
B3LYP*	94.79	82.97	122.28	109.29	88.62	128.00	146.79	121.52	162.50	3.82	6.63
B3LYP54	94.72	84.87	124.18	106.14	86.74	125.32	135.82	111.72	151.42	− 0.16	3.42
B3LYP60	94.67	85.15	124.46	105.63	86.45	124.91	134.16	110.27	149.77	− 0.77	3.39
B3PW91	89.98	73.97	111.29	100.80	78.98	116.97	137.43	110.36	150.02	− 5.84	6.81
B3V5LYP	94.95	83.53	122.86	108.95	88.56	127.85	145.23	120.18	161.00	3.42	6.06
B97-3	95.56	79.92	119.60	109.37	86.86	126.70	145.92	119.03	160.35	2.33	6.10
B98	97.98	82.21	122.21	109.84	87.76	127.56	147.14	121.17	162.06	3.95	6.09
HFLYP	93.94	82.37	119.89	102.92	83.23	120.65	124.41	100.59	138.63	− 6.20	6.26
HFPW91	87.83	70.59	105.68	92.92	71.59	107.41	113.88	88.03	124.70	− 17.75	17.75
MPW1K	89.39	72.95	109.60	98.63	76.92	114.30	130.19	103.32	142.24	− 9.43	9.43
MPW1PW91	89.78	73.62	110.77	100.35	78.60	116.45	135.40	108.35	147.91	− 6.79	6.92
MPW3LYP	95.78	84.45	123.95	110.33	89.88	129.37	145.86	120.86	161.89	4.44	6.89
MPWLYP1M	96.34	86.10	126.30	112.35	92.31	132.33	150.82	126.16	167.85	7.58	9.90
O3LYP	98.23	84.39	123.18	105.27	84.66	122.07	138.66	112.81	151.88	− 0.14	3.08
PBE1	90.89	74.46	112.00	101.76	79.95	118.11	136.46	109.51	149.35	− 5.54	6.17
Range-separated GGA											
CAM-B3LYP	95.63	83.55	122.74	109.06	88.64	128.08	143.34	118.41	159.70	2.97	5.49
HSE	90.54	74.44	111.85	101.97	80.18	118.42	137.65	110.93	151.04	− 5.04	6.36
LC-MPWLYP	95.32	82.67	122.34	108.40	88.03	127.98	140.73	115.93	158.40	1.94	4.61
LC-OLYP	96.60	82.89	122.04	107.82	87.33	126.41	138.36	113.44	154.83	0.82	3.27
LC-OPBE	90.38	70.92	107.53	97.28	75.16	112.57	128.01	100.74	140.63	− 11.02	11.02
LC-ωPBE	90.07	73.15	111.56	97.26	75.83	114.37	130.72	103.80	145.40	− 8.91	8.91
ωB97X	91.20	75.87	111.50	105.22	83.65	121.10	149.87	126.45	166.55	1.00	9.99
Range-separated GGA-D											
ωB97X-D	87.64	71.63	106.79	100.28	78.33	115.40	145.72	121.07	160.24	− 3.92	11.24
Meta-GGA											
M06-L	90.35	76.86	114.23	106.22	82.61	121.71	148.08	122.52	162.26	0.27	8.34
TPSS	93.08	81.92	120.42	101.42	82.19	120.12	138.20	112.02	151.79	− 2.36	4.12
VS98	98.52	77.46	113.20	103.68	80.06	117.13	145.49	120.06	155.97	− 1.20	7.30
Hybrid meta-GGA											
BMK	91.63	75.10	115.60	107.79	83.53	124.47	153.41	126.53	168.33	2.67	9.61
M05	107.31	92.14	134.49	114.76	93.52	135.05	158.82	136.00	179.08	14.31	14.31
M05-2X	109.06	91.59	134.52	120.31	97.16	137.82	144.03	119.44	158.31	9.97	9.97
M06	96.37	81.61	119.49	110.59	88.48	129.00	158.13	132.60	173.56	7.49	10.73
M06-2X	106.00	87.84	129.77	115.75	90.83	130.35	139.26	111.87	151.89	4.58	4.75
M06-HF	117.51	97.01	141.90	114.85	91.44	129.31	115.01	84.22	122.69	− 0.94	15.10
M08-HX	102.81	83.89	123.83	110.55	86.74	127.00	137.61	109.67	150.84	1.17	2.15
M08-SO	105.17	87.86	127.36	113.97	91.64	134.01	142.23	117.45	159.03	6.26	6.62

TABLE V. (*Continued*)

	B^+	B	C^+	Al^+	Al	Si^+	Ga^+	Ga	Ge^+		
Expt.[b]	106.78	82.35	122.92	107.27	82.98	126.00	138.05	108.69	147.34	MSE	MUE
MPW1KCIS	93.30	75.39	113.58	105.46	82.01	120.63	142.49	115.07	155.42	− 2.11	6.31
MPWKCIS1K	92.80	74.36	111.84	103.02	79.49	117.43	135.00	107.70	147.12	− 5.96	5.96
PW6B95	96.06	79.46	119.27	106.85	83.33	122.63	143.04	115.83	156.53	0.07	4.75
PWB6K	95.17	77.73	116.95	104.66	80.83	119.63	137.43	110.12	150.22	− 3.29	4.25
τHCTHhyb	98.97	83.24	122.76	110.67	88.77	128.15	150.41	125.71	166.34	5.85	7.62
TPSS1KCIS	91.22	76.82	115.32	100.93	79.25	117.07	136.78	109.60	149.14	− 5.14	5.74
TPSSh	93.13	81.43	119.62	101.03	81.63	119.38	135.91	109.81	149.33	− 3.46	4.15

[a]All the calculations were performed with DKH Hamiltonian and cc-pVQZ-DK basis set except CCSD(T), which were performed with DKH Hamiltonian and cc-pV5Z-DK basis set.

[b] Experimental values are spin-orbital-free excitation energies averaged over all *J* values.

excitation energies of the third row elements (Ga and Ge). The OPBE functional *always* underestimates the excitation energies for the V9 database.

The tested GGA functionals tend to have different behaviors determined mainly by their correlation functionals. In the nine tested GGA xc functionals, there are only three correlation functionals, LYP, PW91, and PBE, and, as already mentioned, the PW91 and PBE correlation functionals are almost identical. The GGAs with the LYP correlation functional tend to favor the low-spin states, and the GGAs with the PBE or PW91 correlation functional tend to favor the high-spin states. This can be seen clearly from the comparison of BLYP and BPW91, or OLYP and OPBE. The OLYP yields the best performance for valence excitations in the V9 database, in agreement with its good performance for spin splitting in studies of iron complexes.[50–52,54] The MOHLYP functional, using a modified OptX exchange to fulfill the uniform electron gas limit and one half of the LYP correlation, was previously developed[77] to improve the OLYP functional for transition metal systems. It is encouraging to see the good performance of MOHLYP for the valence excitation energies in the V9 database, with an MUE smaller than all other tested GGA functionals except OLYP.

Unlike the GGA functionals, which have different behaviors according to their correlation functionals, the hybrid GGA functionals have more uniform performance. The MUEs of most hybrid functionals for the valence excitation are around 6 kcal/mol. For GGA functionals that overestimate the valence excitation energies, like BLYP (MUE = 9 kcal/mol) and mPWLYP (MUE = 11 kcal/mol), the inclusion of some portion of Hartree–Fock exchange does lower the high-spin/low-spin energy gaps, in particular for the excitation energies in the V9 database, and this reduces the errors by about 3–4 kcal/mol, as illustrated by the MUEs of B3LYP (6 kcal/mol) and MPW3LYP (7 kcal/mol). By including Hartree–Fock exchange, the hybrid functionals always yield more negative MSEs than their parent local functionals, which means that, for reasons already explained, Hartree–Fock exchange favors high-spin states relative to low-spin states, thus reducing the calculated excitation energies.

Based on the observation that the high-spin/low-spin energy gaps seem to depend almost linearly on the percentage of Hartree–Fock exchange in hybrid functionals for the iron complexes studied, Reiher and coworkers proposed a functional called B3LYP* with reduced percentage of Hartree–Fock exchange for the spin-states energetics.[44] However, B3LYP* does not yield better performance over B3LYP for the valence excitation energies in the V9 database. On the other hand, B3LYP54 and B3LYP60, which have higher percentages of Hartree–Fock exchange, yield much better performance. This shows that the percentage of Hartree–Fock exchange that gives the best result is system-dependent.

For the range-separated functionals, the performance for the valence excitation energies in the V9 database is sometimes very poor, even worse than SVWN. The long-range corrected functionals LC-OPBE and LC-ωPBE, like the exchange-only methods, always underestimate the excitation energies for all tested cases. On the other hand, the LC-MPWLYP and LC-OPBE functionals perform well for the V9 database, with MUEs of 5 and 3 kcal/mol.

The best performance for the excitation energies of the V9 database is obtained by the hybrid meta-GGA functional M08-HX, with an MUE of 2.2 kcal/mol which is even smaller than that of CCSD(T). This agrees with an earlier study[104] of multiplicity-changing excitation energies. The TPSS meta-GGA functional and its hybrid form TPSSh, also perform well for the valence excitations with nearly equal MUEs (about 4 kcal/mol). Both PW6B95 and PWB6K, with very few parameters compared to the later Minnesota functionals, yield quite reasonable excitation energies, with MUEs of 5 and 4 kcal/mol. The M06-2X functional also performs well for the V9 database. The meta-GGA and hybrid meta-GGA functionals with lower percentages of Hartree–Fock exchange, such as M06, M05, and M06-L, are of special interest because they perform well for catalytic databases including transition metals[110] but they all give quite large errors for the high-spin/low-spin excitation energies. Some of them have errors even larger than that of the simple SVWN. This is a clear indication that further work must be done to develop functionals suitable for the study of chemical reactions involving spin changes during the reaction process.

2. Rydberg excitations

For the Rydberg excitations in the R8 database, Table VI shows that the exchange-only methods again strongly underestimate the excitation energies. The calculated errors of

TABLE VI. The performance of relativistic ΔSCF calculations with various functionals for the Rydberg excitations of the R8 database (kcal/mol).[a]

	F	Ne	Ne^+	Cl	Ar	Br	Kr	Kr^+		
Expt.[b]	292.88	384.58	626.93	205.81	268.12	180.89	233.56	321.91	MSE	MUE
CCSD(T)	291.60	382.90	624.96	204.69	266.54	182.12	233.26	323.79	−0.60	1.38
Exchange only										
B88	270.62	358.14	600.36	181.85	241.17	158.23	207.07	296.39	−25.11	25.11
HF	256.25	343.39	594.51	184.92	245.52	164.09	215.08	308.71	−25.28	25.28
OptX	267.15	359.96	599.55	183.75	245.65	158.18	209.93	298.80	−23.96	23.96
LSDA										
SPL	301.70	392.97	632.71	207.66	267.54	183.52	231.95	324.99	3.55	4.09
SPWL	300.35	392.17	631.24	206.61	266.85	182.56	231.29	321.47	2.23	3.23
SVWN	304.18	395.61	634.99	209.58	269.76	185.24	236.41	324.00	5.64	5.64
GGA										
BLYP	296.52	381.35	626.19	203.58	260.68	179.35	225.57	317.68	−2.97	3.88
BPW91	295.30	382.13	627.60	204.81	263.91	179.91	228.56	319.66	−1.60	2.37
MOHLYP	288.93	377.12	619.28	202.60	261.30	176.83	225.32	317.08	−5.78	5.78
mPWLYP	296.61	381.38	625.94	203.28	260.34	179.10	225.21	317.14	−3.21	4.14
OLYP	293.26	383.53	625.55	205.74	265.60	179.59	228.99	320.40	−1.50	1.60
OPBE	291.31	383.57	626.29	206.75	268.52	180.07	231.82	321.02	−0.67	1.00
PBE	293.55	380.30	624.46	202.94	262.05	178.09	226.63	317.27	−3.67	3.84
PW91	295.32	382.18	626.78	204.01	263.08	179.18	227.65	318.34	−2.27	2.88
RPBE	291.39	377.57	622.44	202.56	261.39	177.27	225.86	316.88	−4.91	4.91
Hybrid GGA										
B3LYP	295.20	380.57	627.00	205.58	263.52	181.73	228.98	321.47	−1.33	2.14
B3LYP*	295.82	381.53	627.12	205.32	263.27	181.40	228.56	320.80	−1.36	2.27
B3LYP54	291.27	374.27	626.37	207.46	265.10	184.10	231.71	326.07	−1.04	3.30
B3LYP60	290.63	373.19	626.29	207.80	265.36	184.53	232.17	326.88	−0.98	3.63
B3PW91	293.61	380.67	627.56	206.10	265.66	181.79	230.99	322.71	−0.70	1.54
B3V5LYP	294.46	379.92	626.29	204.98	262.95	181.19	228.44	320.96	−1.94	2.41
B97-3	298.00	384.47	633.40	211.24	270.26	184.97	234.29	327.03	3.62	3.65
B98	296.65	384.41	632.23	209.94	269.23	185.44	234.38	327.61	3.15	3.19
HFLYP	282.81	367.55	620.59	207.20	266.07	185.75	234.65	330.26	−2.47	6.40
HFPW91	282.22	368.85	622.68	208.87	269.58	186.92	238.02	332.84	−0.59	7.07
MPW1K	289.24	376.01	625.03	206.24	266.25	182.62	232.54	324.94	−1.48	2.77
MPW1PW91	291.70	378.48	625.93	205.48	265.15	181.34	230.75	322.49	−1.67	1.93
MPW3LYP	294.35	379.65	625.93	204.93	262.83	181.24	228.41	320.85	−2.06	2.52
MPWLYP1M	295.81	380.58	625.61	203.44	260.64	179.39	225.70	317.78	−3.22	3.95
O3LYP	293.19	383.04	626.47	206.56	266.54	180.96	230.48	322.42	−0.63	1.04
PBE1	290.14	376.93	623.58	204.25	263.98	180.15	229.58	321.13	−3.12	3.12
Range-separated GGA										
CAM-B3LYP	296.48	382.01	627.18	207.55	265.44	183.96	231.02	323.91	0.36	2.31
HSE	290.43	377.02	623.85	203.86	263.52	180.17	229.06	320.84	−3.24	3.24
LC-MPWLYP	303.92	390.57	633.41	211.56	269.35	188.09	234.66	329.31	5.77	5.77
LC-OLYP	300.47	390.65	629.79	211.04	270.22	187.12	234.89	328.68	4.77	4.77
LC-OPBE	298.82	391.07	630.67	212.30	273.46	187.94	238.13	331.00	6.09	6.09
LC-ωPBE	300.09	386.56	633.44	210.67	269.70	185.90	234.24	328.64	4.32	4.32
ωB97X	299.53	386.86	635.63	213.65	272.92	189.40	236.12	325.50	5.62	5.62
Range-separated GGA-D										
ωB97X-D	297.83	385.46	635.57	211.84	271.29	187.14	234.75	329.76	4.87	4.87
Meta-GGA										
M06-L	303.14	389.35	641.85	218.29	282.00	189.75	238.02	333.68	10.18	10.18
TPSS	292.54	380.47	625.56	207.02	266.35	183.42	232.38	324.61	−0.29	1.90
VS98	297.06	390.86	636.01	210.80	271.25	184.68	234.45	328.98	4.93	4.93
Hybrid meta-GGA										
BMK	298.38	384.09	632.80	210.70	270.94	183.56	232.23	325.07	2.89	3.34
M05	297.43	388.53	635.88	209.64	273.24	184.78	230.83	327.78	4.18	4.86
M05-2X	299.04	387.86	633.58	213.05	271.96	190.82	240.90	333.43	7.00	7.00
M06	301.87	392.30	641.18	210.32	273.34	183.08	231.27	325.09	5.47	6.04
M06-2X	296.26	381.95	628.80	209.26	268.46	181.03	231.57	321.92	0.57	1.73
M06-HF	289.63	377.12	621.05	206.06	260.14	183.40	234.91	323.36	−2.38	3.77
M08-HX	293.32	382.01	629.54	207.39	266.67	186.33	237.61	327.85	2.01	3.01
M08-SO	294.33	382.16	629.45	205.08	265.41	181.54	231.24	320.83	−0.58	1.74

TABLE VI. (*Continued*)

	F	Ne	Ne^+	Cl	Ar	Br	Kr	Kr^+		
Expt.[b]	292.88	384.58	626.93	205.81	268.12	180.89	233.56	321.91	MSE	MUE
MPW1KCIS	294.59	381.06	627.62	204.28	263.69	179.00	227.77	319.03	− 2.21	2.81
MPWKCIS1K	290.95	377.43	626.26	205.38	265.38	180.81	230.43	322.55	− 1.94	2.10
PW6B95	294.22	382.14	628.89	206.54	266.57	182.28	231.22	323.73	0.11	1.70
PWB6K	290.73	379.07	626.83	206.54	267.27	182.80	232.46	325.47	− 0.44	1.99
τHCTHhyb	299.14	388.83	635.94	212.42	272.56	189.39	237.89	331.36	6.61	6.61
TPSS1KCIS	292.19	379.16	625.98	205.90	265.15	181.22	230.20	322.53	− 1.54	1.80
TPSSh	291.33	379.19	625.17	207.21	266.78	183.82	233.10	325.57	− 0.31	2.31

[a]All the calculations were performed with DKH Hamiltonian and d-aug-cc-pVQZ-DK basis set except CCSD(T), which were performed with DKH Hamiltonian and d-aug-cc-pV5Z-DK basis set.

[b]Experimental values are spin-orbital-free excitation energies averaged over all *J* values.

OptX can be reduced to less than 2 kcal/mol by adding either LYP or PBE correlation, with similar trends observed for B88 and HF. The great reduction of the calculated error by adding correlation functionals indicates the importance of dynamic correlation in the correct description of multiplicity-changing excitation energies. Unlike the case for valence excitation energies in the V9 database, the general trends for Rydberg excitation energies in the R8 database are not so sensitive to the choice of correlation functional, as one can see from the comparison of BLYP to BPW91, OLYP to OPBE, and HFLYP to HFPW91. The calculated errors of various density functionals for Rydberg excitation energies are much smaller than those in the V9 database.

The LSDA functionals, namely, SPL, SPWL, and SVWN, favor low-spin ground states relative to high-spin Rydberg states and give positive MSEs. All tested GGA functionals tend to underestimate the Rydberg excitation energies as shown by the negative MSEs. MOHLYP and RPBE functionals *always* underestimate the excitation energies, as seen by the MSE being precisely the negative of the MUE in Table VI. The GGA functionals perform well for the Rydberg excitation energies, with the best performance obtained by OPBE (MUE = 1.0 kcal/mol). The performance of OLYP is also quite good, with an MUE of 1.6 kcal/mol. It is worth pointing out that the best performing functionals have MUEs similar to CCSD(T).

By including a portion of Hartree–Fock exchange, the hybrid GGA functionals improve the performances of ΔSCF calculations for Rydberg excitations over that of the local functionals. However, the hybrid GGA functionals B97-3 and B98, which have reasonably good accuracy for the thermochemistry of closed-shell molecules, do not provide satisfactory results in this case, and are among the worst hybrid GGA functionals for the R8 database. Once again, the B3LYP* functional, designed to improve the performance for spin energetics, does not yield any improvement over the original B3LYP. Unlike for the case of the V9 database, the performance of B3LYP54 and B3LYP60, which have higher percentages of Hartree–Fock exchange, is worse than that of B3LYP and B3LYP* for the R8 database.

Local functionals do not seem to have large deficiencies for describing Rydberg excitations with the △SCF approach, since most functionals have MUEs smaller than 4 kcal/mol. All LSDA and GGA functionals give quite good results for the atomic Rydberg excitations.

Table VI shows that meta-GGA and hybrid meta-GGA functionals do not seem to improve the performance for Rydberg excitation over the best performing GGA and hybrid-GGA functionals. However, three functionals stand out, for especially good performance in absolute terms, namely, M06-2X, M08-SO, and PW6B95, with MUEs close to 1.7 kcal/mol. Five other hybrid meta-GGA functionals also have MUEs below 2.5 kcal/mol: TPSS1KCIS (MUE = 1.8 kcal/mol), TPSS (MUE = 1.9 kcal/mol), PWB6K (MUE = 2.0 kcal/mol), MPWKCIS1K (MUE = 2.1 kcal/mol), and TPSSh (MUE = 2.3 kcal/mol). M08-HX, which is the best hybrid meta-GGA functional for valence excitations, gives acceptable results for Rydberg excitation, with an MUE of 3.0 kcal/mol.

3. Overall performance

The overall performance of various density functionals for valence and Rydberg excitations calculated with the ΔSCF method is summarized in Table VII. Our results show that Rydberg excitations of p-block atoms and cations are, in fact, well described by most tested functionals, which may be contrary to some expectations. However, the valence excitations in the V9 database represent a harder test for the current functionals. Several widely used functionals, e.g., PBE, PW91, B3LYP, PBE1, M06, and M06-L, have MUEs larger than 6.0 kcal/mol for valence excitations. The best functional for combined valence and Rydberg excitations is the O3LYP hybrid GGA functional, which has an MUE (2.1 kcal/mol) comparable to that of CCSD(T) (2.0 kcal/mol). The M08-HX and OLYP functionals also perform well, with MUEs of 2.6 and 2.7 kcal/mol. Other functionals with MUEs below 4 kcal/mol are: TPSS (3.0), PWB6K (3.2), PW6B95 (3.2), TPSSh (3.2), M06-2X (3.2), B3LYP54 (3.4), B3LYP60 (3.5), TPSS1KCIS (3.8), and CAM-B3LYP (3.9). It is encouraging to see that many meta-GGA and hybrid meta-GGA functionals perform well for valence and Rydberg excitations, which confirms the efficacy of including kinetic energy density into the functional forms. However, it is disappointing to see that the functionals such as M06, M05, M06-L, τHCTHhyb, and ωB97X-D,

TABLE VII. The overall performance of relativistic ΔSCF calculations with various functionals for valence and Rydberg excitations in the VR17 database (kcal/mol).

	V9		R8		VR17	
	MSE	MUE	MSE	MUE	MSE	MUE
CCSD(T)	− 2.41	2.71	− 0.60	1.38	− 1.51	2.04
Exchange only						
B88	− 19.50	19.50	− 25.11	25.11	− 22.30	22.30
HF	− 32.53	32.53	− 25.28	25.28	− 28.90	28.90
OptX	− 25.26	25.26	− 23.96	23.96	− 24.61	24.61
LSDA						
SPL	2.19	8.78	3.55	4.09	2.87	6.44
SPWL	1.74	8.48	2.23	3.23	1.99	5.85
SVWN	1.12	8.85	5.64	5.64	3.38	7.24
GGA						
BLYP	6.66	9.25	− 2.97	3.88	1.85	6.56
BPW91	− 4.71	8.32	− 1.60	2.37	− 3.15	5.35
MOHLYP	2.45	4.15	− 5.78	5.78	− 1.66	4.96
mPWLYP	8.31	10.61	− 3.21	4.14	2.55	7.38
OLYP	0.87	3.79	− 1.50	1.60	− 0.32	2.69
OPBE	− 10.94	10.94	− 0.67	1.00	− 5.80	5.97
PBE	− 1.30	6.99	− 3.67	3.84	− 2.49	5.42
PW91	− 1.37	6.94	− 2.27	2.88	− 1.82	4.91
RPBE	− 1.21	5.10	− 4.91	4.91	− 3.06	5.01
Hybrid GGA						
B3LYP	3.30	6.05	− 1.33	2.14	0.99	4.09
B3LYP*	3.82	6.63	− 1.36	2.27	1.23	4.45
B3LYP54	− 0.16	3.42	− 1.04	3.30	− 0.60	3.36
B3LYP60	− 0.77	3.39	− 0.98	3.63	− 0.87	3.51
B3PW91	− 5.84	6.81	− 0.70	1.54	− 3.27	4.17
B3V5LYP	3.42	6.06	− 1.94	2.41	0.74	4.23
B97-3	2.33	6.10	3.62	3.65	2.98	4.88
B98	3.95	6.09	3.15	3.19	3.55	4.64
HFLYP	− 6.20	6.26	− 2.47	6.40	− 4.34	6.33
HFPW91	− 17.75	17.75	− 0.59	7.07	− 9.17	12.41
MPW1K	− 9.43	9.43	− 1.48	2.77	− 5.45	6.10
MPW1PW91	− 6.79	6.92	− 1.67	1.93	− 4.23	4.42
MPW3LYP	4.44	6.89	− 2.06	2.52	1.19	4.70
MPWLYP1M	7.58	9.90	− 3.22	3.95	2.18	6.92
O3LYP	− 0.14	3.08	− 0.63	1.04	− 0.38	2.06
PBE1	− 5.54	6.17	− 3.12	3.12	− 4.33	4.64
Range-separated GGA						
CAM-B3LYP	2.97	5.49	0.36	2.31	1.66	3.90
HSE	− 5.04	6.36	− 3.24	3.24	− 4.14	4.80
LC-MPWLYP	1.94	4.61	5.77	5.77	3.86	5.19
LC-OLYP	0.82	3.27	4.77	4.77	2.80	4.02
LC-OPBE	− 11.02	11.02	6.09	6.09	− 2.47	8.55
LC-ωPBE	− 8.91	8.91	4.32	4.32	− 2.30	6.62
ωB97X	1.00	9.99	5.62	5.62	3.31	7.80
Range-separated GGA-D						
ωB97X-D	− 3.92	11.24	4.87	4.87	0.48	8.06
Meta-GGA						
M06-L	0.27	8.34	10.18	10.18	5.22	9.26
TPSS	− 2.36	4.12	− 0.29	1.90	− 1.33	3.01
VS98	− 1.20	7.30	4.93	4.93	1.86	6.11
Hybrid meta-GGA						
BMK	2.67	9.61	2.89	3.34	2.78	6.48
M05	14.31	14.31	4.18	4.86	9.24	9.59
M05-2X	9.97	9.97	7.00	7.00	8.48	8.48
M06	7.49	10.73	5.47	6.04	6.48	8.39
M06-2X	4.58	4.75	0.57	1.73	2.58	3.24
M06-HF	− 0.94	15.10	− 2.38	3.77	− 1.66	9.43
M08-HX	1.17	2.15	2.01	3.01	1.59	2.58
M08-SO	6.26	6.62	− 0.58	1.74	2.84	4.18
MPW1KCIS	− 2.11	6.31	− 2.21	2.81	− 2.16	4.56
MPWKCIS1K	− 5.96	5.96	− 1.94	2.10	− 3.95	4.03
PW6B95	0.07	4.75	0.11	1.70	0.09	3.22
PWB6K	− 3.29	4.25	− 0.44	1.99	− 1.86	3.12
τHCTHhyb	5.85	7.62	6.61	6.61	6.23	7.11
TPSS1KCIS	− 5.14	5.74	− 1.54	1.80	− 3.34	3.77
TPSSh	− 3.46	4.15	− 0.31	2.31	− 1.89	3.23

which have been recently shown to perform quite well for a diverse database relevant to catalysis, do not perform well for multiplicity-changing valence and Rydberg excitation energies. This emphasizes the need of further work to better balance exchange and correlation functionals, in order to obtain a correct description of the multiplicity-changing excitations. The VR17 database can serve as a database for such purpose of training or testing new functionals in the future; and the representative databases to be introduced in Sec. VIII will be even more convenient than this.

B. Low-spin time-dependent DFT

Many researchers have pointed out that LS-TDDFT has serious problems for Rydberg excitations with local functionals. When a local functional is used, LS-TDDFT usually significantly underestimates the Rydberg excitation energies.[102,112,144] The failure of LS-TDDFT with local functionals has been attributed to the failure of approximate functionals to produce the correct Coulomb-like behavior far from the nucleus. By using the range-separated hybrid approach to introduce 100% Hartree–Fock exchange for large interelectronic distances, the resulting long-range corrected functionals can reproduce the correct asymptotic behavior. In fact some of the range-separated functionals were specifically developed with the aim of giving improved performance for Rydberg and charge-transfer excitations. Previous LS-TDDFT studies on small molecules has shown the improved performance of long-range corrected functionals for Rydberg excitations.[112] Table VIII shows that the long-range corrected functionals, which are designed to improve the performance for Rydberg excitations, in fact, perform worse than the original GGAs for the R8 database.

The different performance of long-range corrected functionals in the present study and the previous studies might be due to the differences between the LS-TDDFT and ΔSCF approaches. However, in our tested cases, the ΔSCF approach has a more-solid-than-usual theoretical foundation since the ground states and excited states in our test cases are the lowest energy states of their spin symmetry, and they are well represented by single Slater determinants. The Kohn–Sham formalism can be applied to such systems without any con-

TABLE VIII. Comparison of LS-TDDFT and △SCF calculated Rydberg excitation energies with d-aug-cc-pVQZ basis set.[a]

	Ne	Ar	Kr	MSE	MUE
LS-TDDFT with d-aug-cc-pVQZ-DK					
HF	414.06	272.62	234.36	11.59	11.59
B88	286.46	207.86	181.14	−70.27	70.27
SVWN	321.88	238.25	210.17	−38.65	38.65
PBE	307.42	228.11	200.49	−50.08	50.08
B3LYP	332.90	239.30	209.26	−34.93	34.93
M06-L	315.83	219.61[b]	211.71	−46.37	46.37
M06	318.61	226.37	198.53	−47.59	47.59
LC-ωPBE	330.81	254.44	224.95	−25.35	25.35
HSE	342.86	246.99	215.73	−26.89	26.89
ωB97X-D	335.51	246.96	217.91	−28.63	28.63
O3LYP	316.78	230.84	202.41	−45.41	45.41
OLYP	297.97	220.37	193.62	−58.10	58.10
M08-HX	350.31	241.09	206.95	−29.30	29.30
B3LYP54	375.59	260.90	226.71	−7.69	7.69
B3LYP60	383.00	264.61	229.71	−2.98	2.98
△SCF with d-aug-cc-pVQZ-DK					
HF	343.39	245.52	215.08	−27.43	27.43
B88	358.14	241.17	207.07	−26.62	26.62
SVWN	395.61	269.76	236.41	5.17	5.17
PBE	380.30	262.05	226.63	−5.76	5.76
B3LYP	380.57	263.52	228.98	−4.40	4.40
M06-L	389.35	282.00	238.02	7.70	7.70
M06	392.30	273.34	231.27	3.55	5.08
LC-ωPBE	386.56	269.70	234.24	1.41	1.41
HSE	377.02	263.52	229.06	−5.55	5.55
ωB97X-D	385.46	271.29	234.75	1.75	1.75
O3LYP	383.04	266.54	230.48	−2.07	2.07
OLYP	383.53	265.60	228.99	−2.72	2.72
M08-HX	382.01	266.67	237.61	0.01	2.69
B3LYP54	374.27	262.83	228.41	−6.92	6.92
B3LYP60	373.19	265.36	232.17	−5.18	5.18

[a]All the calculations were performed with DKH Hamiltonian.
[b]Calculation with a pruned (99, 590) grid (ultrafine grid) fails to converge; this value is obtained with a pruned (75, 302) grid (fine grid).

ceptual problem. The only approximation we introduced is the approximate exchange-correlation functional. So the performance of each functional will directly reflect how well the functional balances exchange and correlation. On the other hand, LS-TDDFT calculations may introduce errors both from the approximations of the adiabatic linear response scheme and from the approximate functionals. As pointed out in a recent study of core excited states, core excitation energies are systematically underestimated by LS-TDDFT calculations, while the excitation energies obtained by △SCF agree well with experimental values.[145]

According to our basis set study, a doubly augmented basis set is required to correctly describe the Rydberg excitations. We performed LS-TDDFT calculations with 15 different functionals with d-aug-cc-pVQZ-DK basis set for Ne, Ar, and Kr atoms, and the results are shown in Table VIII. With the d-aug-cc-pVQZ-DK basis set, the LS-TDDFT method *always* underestimates the Rydberg excitation energies, even for the long-range corrected functionals, namely, LC-ωPBE and ωB97X-D, which have the correct long-range asymptotic behavior and are designed for Rydberg and charge-transfer excitations. On the other hand, time-dependent Hartree–Fock theory always overestimates the Rydberg excitation energies. B3LYP54 and B3LYP60, two modifications of B3LYP obtained by rising the percentage of Hartree–Fock exchange, yield acceptable Rydberg excitation energies; the B3LYP54 and B3LYP60 functionals do not have the correct long-range asymptotic behavior, so the good performance of B3LYP54 and B3LYP60 might be a result of the cancellation of errors. We note that the statistical average orbital parameters potential,[146,147] which is a model potential with the correct $-1/r$ asymptotic behavior, gives good performance for Rydberg excitations,[147,148] but it is not included in the present study.

The underestimation of Rydberg excitation energies by most tested functionals in the present work, combined with the fact that ΔSCF calculations do much better with the same functionals, suggests that the poor performance of LS-TDDFT for the Rydberg excitations might not be a result of the approximate functionals but a result of the adiabatic linear response scheme in LS-TDDFT. A recent finding consistent with this point of view is that by modifying the linear response scheme of LS-TDDFT, the description of Rydberg excitations can be improved greatly even with an LSDA functional.[149,150] Also in agreement with the trend of our results, but interpreting the results more narrowly, a recent TDDFT study[151] of ethylene showed strong underestimation of the singlet-triplet excitation energy and attributed the disappointing performance solely to the adiabatic approximation.

Besides Rydberg excitations, charge-transfer excitations are also notoriously difficult for conventional linear response TDDFT with local functionals. The failure of local functionals for charge-transfer excitations has also been attributed the incorrect asymptotic behavior of local functionals.[13,152] Ziegler and coworker recently developed a constrained variational density functional theory (CV-DFT) to treat excited states.[153] The adiabatic linear response TDDFT within the Tamm-Dancoff approximation can be derived with CV-DFT approach. They traced the failure of TDDFT for charge-transfer excitations back to the linear response TDDFT formalism rather than the incorrect asymptotic behavior of local functionals.[154] Even with SVWN, which does not have the correct $-1/r$ asymptotic behavior, good performance can be obtained for charge-transfer excitations when one goes beyond the linear response TDDFT.[155] This is consistent with our interpretation in that the failure of TDDFT for Rydberg excitations may be attributed to the adiabatic linear response approximation.

C. Collinear spin-flip time-dependent DFT

Given the failure of LS-TDDFT to describe the Rydberg excitations in the R8 database, it is of interest to see if SF-TDDFT can improve on such results. In Table IX we show the SF-TDDFT excitation energies for the R8 database with d-aug-cc-pVQZ basis sets. The methods in the first column are ordered by the percentage of Hartree–Fock exchange at small interelectronic distances (i.e., X is 0.001 in B3LYP0,

TABLE IX. SF-TDDFT results for Rydberg transitions in the R8 database with d-aug-cc-pVQZ basis set.[a]

	F	Ne	Ne^+	Cl	Ar	Br	Kr	Kr^+	MSE	MUE
B3LYP0	382.05	479.92	732.55	248.21	310.97	217.61	264.51	359.33	60.06	60.06
O3LYP	349.79	447.68	693.62	230.69	294.63	198.30	249.15	335.31	35.56	35.56
B3LYP*	357.54	451.20	706.32	237.75	299.01	209.41	257.20	352.21	44.50	44.50
ωB97X	393.99	470.22	755.50	248.26	301.61	234.50	255.20	352.94	62.19	62.19
B3LYP	351.26	444.02	699.79	235.59	296.35	207.88	256.24	328.23	38.09	38.09
ωB97X-D	389.05	462.74	744.96	248.74	301.66	234.59	257.72	362.98	60.97	60.97
M06	326.55	434.61	708.31	177.72	300.07	216.06	257.71	359.58	33.24	40.26
PWB6K	335.50	411.61	685.31	235.62	295.46	207.81	255.02	352.94	33.07	33.07
M06-2X	321.23	382.70	667.45	216.12	263.99	188.12	230.67	295.50	6.39	15.22
B3LYP54	296.39	379.01	640.07	210.72	268.10	187.91	234.88	326.61	3.63	5.02
B3LYP60	287.21	368.04	629.96	206.60	263.33	184.56	231.27	326.64	− 2.13	5.19
HF	211.90	285.39	549.80	165.48	220.93	154.04	196.52	311.51	− 52.39	52.39

[a]All results in this table include scalar relativistic effects calculated at the ΔSCF level, as listed in Table IV.

11.61 in O3LYP, 15 in B3LYP*, 15.7706 in ωB97X, 20 in B3LYP, 22.0036 in ωB97X-D, 27 in M06, 46 in PWB6K, 54 in M06-2X and B3LYP54, 60 in B3LYP60, and 100 in HF); note that this is also the amount of Hartree–Fock exchange at large interelectronic distances, except for the ωB97X and ωB97X-D long-range corrected functionals, in which the fraction of Hartree-Fock exchange increases with increasing interelectronic distance, eventually reaching 100% at the asymptote. It can be seen that large errors still prevail for most of the functionals. Those functionals with constant and relatively low percentages of Hartree–Fock exchange highly overestimate the excitation energies, and the HF approximation, with no correlation, highly underestimates them. The long-range corrected functionals also strongly overestimate the excitation energies, and in this respect their performance is similar to what would be expected on the basis of their Hartree-Fock exchange percentage at small interelectronic distances, except that it is slightly worse than that. Best results are observed for intermediate values of Hartree–Fock exchange, between 54% and 60%, in qualitative agreement with the previous observation that about 50% exchange was about optimal for singlet–triplet splittings.[19] However, when comparing the MUEs in Tables VI, VIII, and IX, one sees that the level of accuracy attained with B3LYP60/d-aug-cc-pVQZ is worse than that obtained with the LS-TDDFT approach (where only singlet–triplet transitions were considered), and also somewhat worse than that obtained with the ΔSCF approach.

An analogous study has been carried out for the valence excitations in the V9 database, and the results are shown in Table X. Note that the spin-flip calculations fail to provide a reasonable approximation for the low- and high-spin states for the ωB97X, ωB97X-D, M06, and M06-2X calculations on the B atom, and similarly fail for M06-2X calculations on the C^+ cation. Thus, for these cases no results are reported in Table X. From the MSEs and MUEs in the table, one can reach the same conclusions as for the R8 database regarding the large errors for extreme values of Hartree–Fock exchange and the best values for about 60% Hartree–Fock exchange.

It is interesting to compare the results for the V9 database in Table X to those obtained by the ΔSCF method in Table V. The best results for V9 with SF-TDDFT are 5.1 kcal/mol with B3LYP60 with $X = 60$ and 9.6 kcal/mol with B3LYP54 with $X = 54$. These errors are much larger than the best results obtained with ΔSCF (in kcal/mol): 2.2 with M08-HX, 3.1 with O3LYP, 3.3 with LC-OLYP, 3.4 with B3LYP54 and B3LYP60, 3.8 with OLYP, 4.1 with TPSS, and 4.2 with

TABLE X. SF-TDDFT results for valence transitions in the V9 database using the cc-pVQZ basis set.[a]

	B^+	B	C^+	Al^+	Al	Si^+	Ga^+	Ga	Ge^+	MSE	MUE
B3LYP0	131.14	128.20	197.66	133.80	122.98	174.48	172.49	156.23	205.26	44.43	44.43
O3LYP	133.38	127.57	193.06	129.96	119.53	170.91	163.83	144.53	193.75	39.35	39.35
B3LYP*	128.83	118.29	187.60	131.00	115.93	166.69	166.86	146.17	194.89	37.10	37.10
ωB97X	100.57	–	138.43	128.48	122.34	176.19	162.38	149.77	199.96	29.76	31.31
B3LYP	126.65	116.62	203.92	129.29	112.96	162.85	164.21	142.61	190.64	36.37	36.37
ωB97X-D	120.66	–	157.77	128.32	118.60	171.34	162.35	148.38	196.52	32.99	32.99
M06	114.90	–	153.68	119.92	73.37	144.95	167.56	145.66	193.20	21.65	24.05
PWB6K	113.98	95.42	148.54	119.29	98.24	144.62	149.40	125.99	170.12	15.91	15.91
M06-2X	116.42	–	–	125.19	107.21	152.99	129.52	105.99	147.37	9.65	12.86
B3LYP54	111.53	94.62	145.06	113.35	91.46	135.19	142.55	115.70	159.25	9.59	9.59
B3LYP60	107.12	90.43	138.47	110.38	87.77	130.47	138.76	111.19	153.94	5.13	5.13
HF	114.35	61.91	98.78	89.72	62.15	99.00	114.17	82.33	120.47	− 19.94	21.63

[a]All results in this table include scalar relativistic effects calculated at the ΔSCF level, as listed in Table IV.

TABLE XI. Values of $\langle \hat{S}^2 \rangle$ for low-spin and high-spin SF-TDDFT solutions for R8 database.

		F	Ne	Ne^+	Cl	Ar	Br	Kr	Kr^+
Theoretical	LS	0.75	0.00	0.75	0.75	0.00	0.75	0.00	0.75
	HS	3.75	2.00	3.75	3.75	2.00	3.75	2.00	3.75
B3LYP0	LS	0.76	0.00	0.75	0.76	0.00	0.75	0.00	0.75
	HS	1.75	1.00	1.75	1.75	1.00	1.75	1.00	1.75
O3LYP	LS	0.76	0.01	0.76	0.76	0.01	0.76	0.01	0.76
	HS	1.77	1.01	1.77	1.78	1.01	1.78	1.02	1.78
B3LYP*	LS	0.76	0.01	0.76	0.76	0.01	0.76	0.00	0.75
	HS	1.77	1.01	1.78	1.80	1.02	1.81	1.03	1.84
ωB97X	LS	0.76	0.01	0.76	0.76	0.01	0.76	0.01	0.76
	HS	1.76	1.00	1.75	1.76	1.00	1.75	1.00	1.75
B3LYP	LS	0.76	0.01	0.76	0.76	0.01	0.76	0.00	0.76
	HS	1.78	1.02	1.80	1.82	1.03	1.84	1.05	1.75
ωB97X-D	LS	0.76	0.01	0.76	0.76	0.01	0.76	0.01	0.75
	HS	1.75	1.00	1.75	1.75	1.00	1.75	1.00	1.75
M06	LS	0.76	0.01	0.76	0.78	0.00	0.76	0.01	0.75
	HS	1.77	1.01	1.83	3.17	1.00	1.75	1.00	1.75
PWB6K	LS	0.77	0.01	0.76	0.76	0.01	0.76	0.01	0.76
	HS	1.96	1.00	2.07	1.76	1.00	1.75	1.00	1.75
M06-2X	LS	0.78	0.02	0.76	0.76	0.02	0.79	0.02	0.77
	HS	2.92	1.00	3.08	1.76	1.01	3.07	1.01	1.75
B3LYP54	LS	0.78	0.02	0.76	0.77	0.01	0.76	0.01	0.76
	HS	1.88	1.06	1.95	2.01	1.11	2.12	1.15	1.75
B3LYP60	LS	0.78	0.02	0.76	0.77	0.02	0.77	0.01	0.76
	HS	1.91	1.07	2.01	2.08	1.13	2.21	1.18	1.75
HF	LS	0.82	0.05	0.78	0.79	0.03	0.79	0.03	0.77
	HS	3.47	1.56	3.71	3.47	1.47	1.76	1.54	3.78

TABLE XII. Values of $\langle \hat{S}^2 \rangle$ for low-spin and high-spin SF-TDDFT solutions for V9 database.

		B^+	B	C^+	Al^+	Al	Si^+	Ga^+	Ga	Ge^+
Theoretical	LS	0.00	0.75	0.75	0.00	0.75	0.75	0.00	0.75	0.75
	HS	2.00	3.75	3.75	2.00	3.75	3.75	2.00	3.75	3.75
B3LYP0	LS	0.01	0.76	0.76	0.00	0.75	0.75	0.00	0.75	0.75
	HS	1.01	2.72	1.79	1.00	1.79	1.78	1.01	1.80	1.78
O3LYP	LS	0.00	0.76	0.75	0.01	0.76	0.75	0.00	0.76	0.75
	HS	1.55	3.72	3.70	1.41	3.23	3.40	1.77	3.74	3.74
B3LYP*	LS	0.00	0.76	0.76	0.00	0.76	0.75	0.00	0.75	0.75
	HS	1.68	3.76	3.67	1.64	3.69	3.67	1.81	3.73	3.72
ωB97X	LS	0.09	–	0.81	0.08	0.86	0.81	0.02	0.79	0.78
	HS	1.36	–	3.03	1.33	2.92	2.88	1.59	3.02	3.14
B3LYP	LS	0.00	0.76	0.76	0.00	0.76	0.75	0.00	0.75	0.75
	HS	1.28	3.71	3.72	1.75	3.71	3.71	1.88	3.74	3.73
ωB97X-D	LS	0.04	–	0.78	0.04	0.81	0.78	0.01	0.78	0.77
	HS	1.87	–	3.48	1.39	3.17	3.14	1.59	3.04	3.25
M06	LS	0.01	–	0.77	0.01	0.77	0.76	0.01	0.77	0.76
	HS	1.95	–	3.58	1.96	2.71	3.66	1.69	3.36	3.49
PWB6K	LS	0.00	0.77	0.76	0.01	0.76	0.75	0.00	0.75	0.75
	HS	1.99	3.70	3.74	1.92	3.71	3.71	1.88	3.74	3.73
M06-2X	LS	0.22	–	–	0.07	0.86	0.82	0.01	0.77	0.76
	HS	1.06	–	–	1.54	2.79	3.21	1.96	3.66	3.70
B3LYP54	LS	0.00	0.76	0.75	0.00	0.76	0.76	0.00	0.76	0.76
	HS	1.97	3.75	3.75	1.98	3.75	3.75	2.00	3.75	3.75
B3LYP60	LS	0.00	0.76	0.75	0.00	0.76	0.76	0.00	0.76	0.76
	HS	1.99	3.75	3.75	1.99	3.75	3.75	2.00	3.75	3.75
HF	LS	1.00	0.76	0.76	0.00	0.77	0.76	0.01	0.77	0.76
	HS	2.00	3.75	3.75	2.00	3.75	3.75	2.00	3.76	3.75

MOHLYP and TPSSh. For SF-TDDFT, good performance seems to require X in the range 54–60, whereas the best performing functionals in the ΔSCF calculation span a wide range of X, from $X = 0$ for OLYP, TPSS, and MOHLYP to $X = 60$ for B3LYP60.

An important aspect of the SF-TDDFT method is the extent to which it produces solutions adapted to the $\langle \hat{S}^2 \rangle$ operator, where S is the total electron spin. In Tables XI and XII we report the values of $\langle \hat{S}^2 \rangle$ for the atoms in the R8 database and for those in the V9 database, respectively. As observed in Table XI, the doublet and singlet solutions are generally well spin adapted, with maximum values of $\langle \hat{S}^2 \rangle$ of 0.04 and 0.81, as compared to the theoretical spin-adapted values of 0.00 and 0.75. However, this is not the case for the triplet and quartet solutions with $M_S = 0$ and 1/2, respectively, produced by SF-TDDFT from the high-spin reference states. These states should have values of $\langle \hat{S}^2 \rangle$ close to 2.00 and to 3.75, respectively. Instead, many of the values shown in the table for the triplet are close to but larger than 1.00, and those for the doublet are close to but larger than 1.75. Looking at the coefficients in the SF-TDDFT expansions, one observes that these solutions are single-determinantal mixtures of a singlet and a triplet (as $(0.00 + 2.00)/2 = 1.00$) and of two doublets and one quartet (as $(0.75 + 0.75 + 3.75)/3 = 1.75$). The spin-adapted triplet with $M_S = 0$ and the quartet with $M_S = 1/2$ should correctly be linear combinations of two determinants and of the three determinants, respectively (for the latter, see, for example, Refs. 156 and 157). Indeed, as the percentage of Hartree–Fock exchange increases, the solutions tend toward the correct character, and for the HF approximation they are almost the correct linear combinations of determinants. We also note that the $M_S = 0$ and $M_S = 1/2$ solutions are not degenerate with the reference triplet $M_S = 1$ and quartet $M_S = 3/2$ solutions; the energy difference between these pairs of solutions has been called the self-splitting test,[158] and it is supposed to be a measure of the consistency of the SF-TDDFT method. Despite these caveats, we have, for consistency and as is explained in Sec. IV, taken the energy of the $M_S = 0$ solution as the triplet energy and the energy of the $M_S = 1/2$ solution as the quartet energy to calculate the singlet–triplet and doublet–quartet splittings of the atoms.

In Table XII, note that the values of $\langle \hat{S}^2 \rangle$ for the atoms in the V9 database are in much better agreement with their theoretical values than were those for the Rydberg states, which is borne out by the coefficients in the SF-TDDFT expansion.

In SF-TDDFT calculations, many of the solutions are not spin-adapted solutions, and the spin-contamination may temper the reliability of results. In 2007, Vahtras and Rinkevicius proposed a general spin-adapted TDDFT to calculate the excitations to states of arbitrary multiplicity for molecules with open-shell ground states.[159] A more compact spin-adapted TDDFT formalism has been developed by Li and Liu via tensor-coupling scheme.[160,161]

An approach not tested in the present article is noncollinear spin-flip TDDFT, which has shown promising

success[20,28,34,162,163] and would be useful to test in the future.

D. Linear dependence on Hartree–Fock exchange

The LS-TDDFT calculations strongly underestimate the excitation energies of Ne, Ar, and Kr with local functionals, but overestimate those excitation energies with Hartree-Fock. On the other hand, SF-TDDFT strongly overestimates the excitation energies for V9 and R8 databases with those functionals containing relative low HF exchange, but it underestimates those excitation energies with Hartree-Fock. Both methods require about 60% HF exchange to yield reasonable results. The excitation energies calculated with the ΔSCF approach also show a dependence on the percentage of HF exchange in the functionals, which is shown clearly from the calculated excitation energies with B3LYP, B3LYP*, B3LYP54, and B3LYP60 in Tables V and VI.

In order to study the relationship between calculated excitation energies and the percentage of HF exchange, we studied a series of density functionals with the same functional form but various percent of HF exchange, in particular, the B3LYP*X* (*X* is the percentage of HF exchange). Five functionals, namely, B3LYP0 ($X = 0.001$), B3LYP* ($X = 15$), B3LYP ($X = 20$), B3LYP54 ($X = 54$), and B3LYP60 ($X = 60$), were considered for the ΔSCF, LS-TDDFT and SF-TDDFT approaches for both valence and Rydberg excitations. As one can see from Figs. 1 and 2, the calculated excitation energies show excellent linear dependence on the percentage of HF exchange, with squared correlation coefficients R^2 larger than 0.998 for all three approaches. Our results agree with Reiher's observation that the high-spin/low-spin splittings (or excitation energies) calculated with the ΔSCF approach depend linearly on the percentage of HF exchange. Our results show that, the linear dependence of HF exchange is not observed only for the ΔSCF approach, but also holds for the LS-TDDFT and SF-TDDFT approaches.

The calculated excitation energies obtained with the ΔSCF approach are not so sensitive to the percentage of HF exchange *X*, while those obtained with LS-TDDFT and SF-TDDFT show strong dependence on *X*, differing by several tens of kcal/mol for various *X*. The optimum value of *X* is both system-dependent and method-dependent. With the ΔSCF approach, the B3LYP0 functional with zero HF exchange gives the exact excitation energies for B and Ne atoms, but B3LYP*X* cannot get the correct excitation energies for Al and Ar atoms for any *X* in the considered range. With the SF-TDDFT approach, the optimum value of *X* seems to be 70 for B and Al atoms and about 50 for Ne and Ar atoms. About 60% HF exchange is needed to yield the correct excitation energies for Ne and Ar atoms with LS-TDDFT approach. This agrees with the observation that B3LYP60 yields reasonable excitation energies for both LS-TDDFT and SF-TDDFT.

Post-SCF calculations were performed with converged HF, SPWL, PBE, and TPSS densities for HF and all tested functionals. The calculated excitation energies are not very sensitive to the reference densities; in particular, the mean absolute deviations (MADs) of post-SCF excitation energies from the SCF excitation energies are usually less than 0.5 kcal/mol (full details are in supplementary material).[164] Therefore, the linear dependence of calculated ΔSCF excitation energies on the percentage of HF exchange is mainly a result of the linear expression of the HF exchange energy in the exchange-correlation functionals.

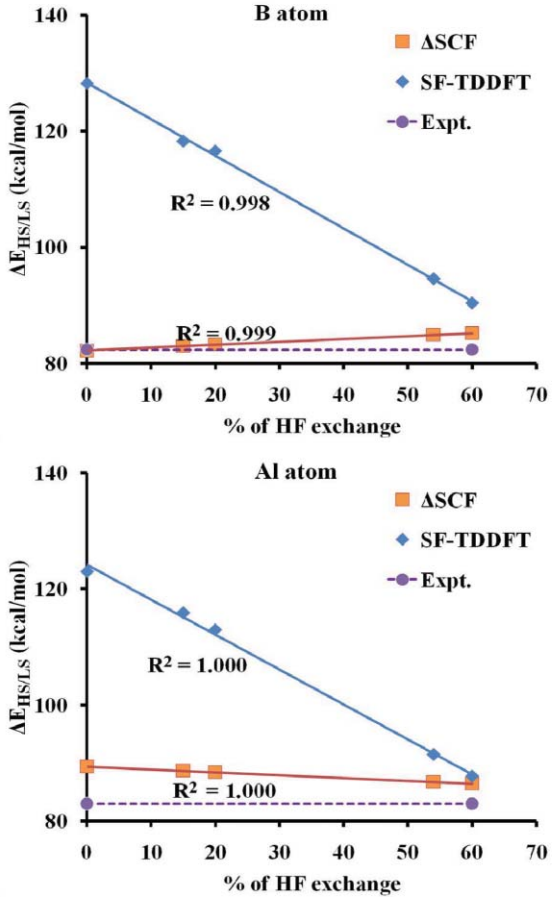

FIG. 1. The dependence of calculated valence excitation energies ($\Delta E_{HS/LS}$) on the percentage of HF exchange in chosen B3LYP*X* (X = 0.001, 15, 20, 54, and 60) series of functionals with ΔSCF and SF-TDDFT approaches.

VIII. REPRESENTATIVE SUBSET

A population sampling script was created and used to select four excitation energies from the V9 database and four from the R8 database, in order to create the R4 and V4 representative subsets. Each subset is chosen such that the mean signed error, the mean unsigned error, and the root-mean-square error for each functional are as close as possible to the corresponding value of the full database, as in previous representative databases.[77,165–167] The ΔSCF/cc-pVQZ-DK, and ΔSCF/d-aug-cc-pVQZ-DK data were used to select the V4 and R4 subsets, respectively. Each subset was then tested, by using the corresponding SF-TDDFT data. The V4 (B, Al^+, Si^+, Ga) and R4 (Ne, Cl, Ar, Br) subsets are presented in Figs. 3 and 4 with a plot of the MUE of HF and 10 DFT functionals for the full database (dot, solid), and the subset (square,

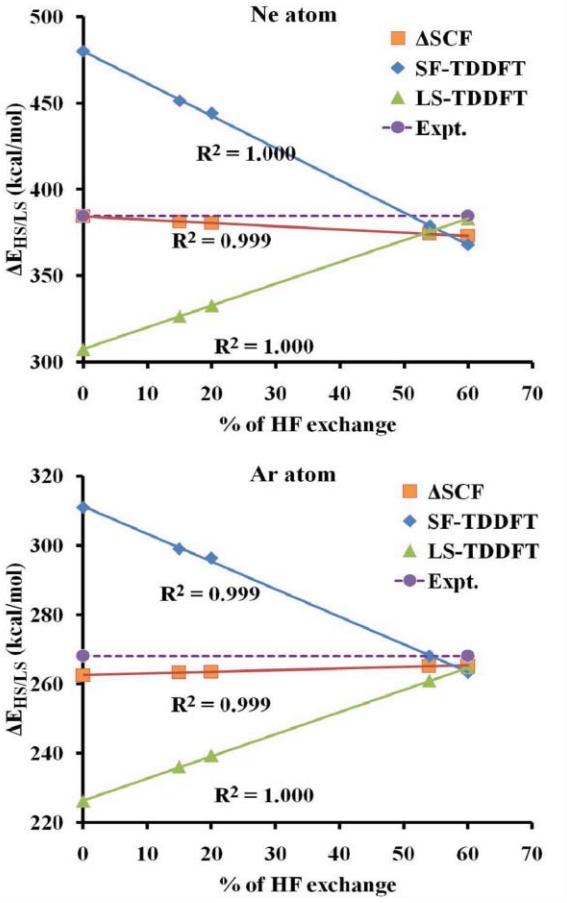

FIG. 2. The dependence of calculated Rydberg excitation energies ($\Delta E_{HS/LS}$) on the percentage of HF exchange in chosen B3LYP*X* (X = 0.001, 15, 20, 54, and 60) series of functionals with ΔSCF, LS-TDDFT, and SF-TDDFT approaches.

dashed), for both ΔSCF and SF-TDDFT. It is clear that there is a very good correspondence between the subset and the full database in both valence excitations (Fig. 3) and Rydberg excitations (Fig. 4).

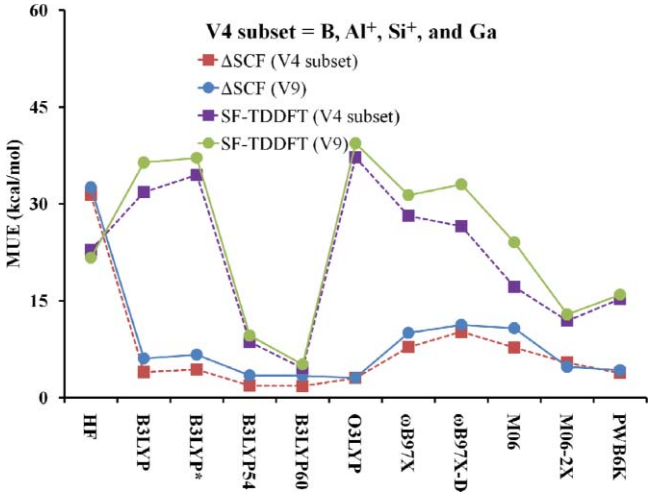

FIG. 3. The mean unsigned errors (MUEs, kcal/mol) of the V4 subset compared to the full V9 database for both ΔSCF and SF-TDDFT results.

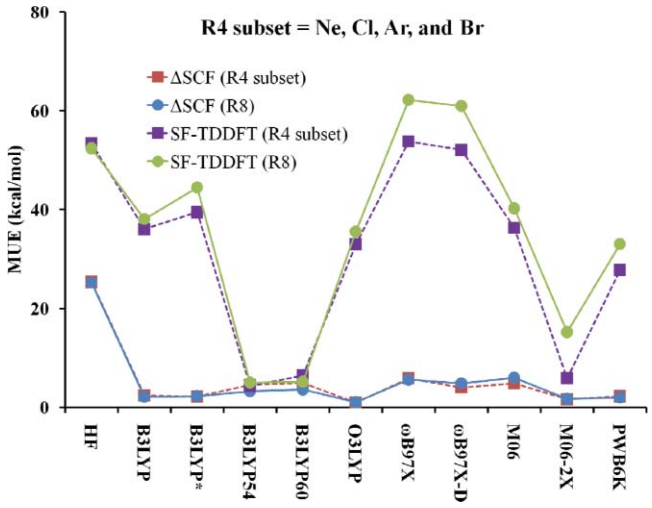

FIG. 4. The mean unsigned errors (MUEs, kcal/mol) of the R4 subset compared to the full R8 database for both ΔSCF and SF-TDDFT results.

IX. CONCLUSIONS

In the present study, a database (VR17) of multiplicity-changing valence and Rydberg excitation energies of the p-block elements is compiled. The VR17 database is composed of 9 multiplicity-changing valence excitations of p-block elements (V9 database), and 8 multiplicity-changing Rydberg excitations of p-block elements (R8 database). Smaller, representative subsets of 4 valence and 4 Rydberg excitations were also sampled and collected in the V4 and R4 subsets, respectively. The VR17 database is built with the guideline of including atoms or cations that have low-spin ground states and high-spin excited states that can be well represented by a single Slater determinant. The ΔSCF approach can be used to extract the excitation energies with more theoretical justification for such transitions. The VR17 database can be used to test the performance of density functionals for spin splittings that are important for understanding reaction mechanisms in organometallics or for studying spin-crossing processes in inorganic chemistry. Perhaps even more importantly, the performance of density functionals for spin splittings provides a fundamental assessment of their ability to provide a balanced treatment of exchange and correlation. The VR17 database, its subdatabases, and representative databases (presented here) can also be used as training sets or validation sets for new density functionals.

A basis set study showed that cc-pVQZ is complete enough to obtain the DFT complete-basis-set limit for the multiplicity-changing valence excitations in the V9 database. The multiplicity-changing Rydberg excitations in the R8 database require much more extensive basis sets. Our results show that a doubly augmented basis set is necessary to yield reliable results for Rydberg excitations.

Even for 3p elements, which are generally not considered to be "heavy" elements, the scalar relativistic effect needs to be considered, especially if quantitative results are required for the excitation energies. The error of the excitation energies due to neglecting scalar relativistic effects is even larger for 4p

elements; it can be up to 9 kcal/mol for monocations and up to 7 kcal/mol for neutral atoms.

For both valence and Rydberg excitations, the excitation energies are strongly underestimated when an exchange-only method, for example, HF, B88, or OptX, is used. Adding a correlation functional improves the performance significantly, highlighting the importance of dynamic correlation in the multiplicity-changing excitations.

The V9 database represents a hard test for approximate functionals since most of them have MUEs larger than 6 kcal/mol. In our ΔSCF results, the best performance for the valence excitation energies is obtained by the hybrid meta-GGA functional M08-HX, with an MUE of 2.2 kcal/mol, even smaller than that of CCSD(T) with a quintuple zeta basis set. The other functionals with MUEs smaller than 5 kcal/mol are: O3LYP (3.1), LC-OLYP (3.3), B3LYP54 (3.4), B3LYP60 (3.4), OLYP (3.8), TPSS (4.1), TPSSh (4.2), PWB6K (4.2), LC-MPWLYP (4.6), PW6B95 (4.8), and M06-2X (4.8).

The errors of various functionals for ΔSCF calculations for the R8 database are much smaller than those for the V9 database. With the ΔSCF approach and the d-aug-cc-pVQZ-DK basis set, the MUEs of most functionals are smaller than 4 kcal/mol (0.2 eV). The OPBE and O3LYP functionals give the smallest MUEs of 1.0 kcal/mol. Other functionals with MUEs smaller than 2.0 kcal/mol are: B3PW91 (1.5), OLYP (1.6), PW6B95 (1.7), M08-SO (1.7), TPSS1KCIS (1.8), TPSS (1.9), and PWB6K (2.0). The M08-HX functional, the best functional for valence excitations, yields an MUE of 3.0 kcal/mol, which is still acceptable for many purposes.

LS-TDDFT calculations with local functionals severely underestimate the excitation energies of Rydberg states, and this has usually been considered to be a deficiency of the density functionals. However, this trend is not observed in our ΔSCF calculations, with many GGA functionals presenting MUEs smaller than 3 kcal/mol. The long-range corrected functionals, which are designed to perform well for Rydberg excitations, yield larger errors than their local parent functionals. A careful comparison of the LS-TDDFT and ΔSCF approaches shows that, when the d-aug-cc-pVQZ-DK basis set is used, the LS-TDDFT calculations underestimate the Rydberg excitation energies by more than 24 kcal/mol (∼1 eV) with most tested density functionals, even the long-range corrected functionals. The poor performance of LS-TDDFT for Rydberg excitation might be a feature of the LS-TDDFT approach itself, rather than a result of incorrect long-range asymptotic behavior in the functionals.

The best overall performance in our ΔSCF calculations is obtained by the O3LYP, M08-HX, and OLYP functionals, with MUEs of 2.1, 2.6 and 2.7 kcal/mol, respectively. The performance of those functionals are encouraging, since the "gold-standard" CCSD(T) with quintuple zeta basis set has an MUE of 2.0 kcal/mol. The TPSS, PWB6K, PW6B95, TPSSh, M06-2X, B3LYP54, B3LYP60, and TPSS1KCIS functionals also perform well, with MUEs smaller than 4 kcal/mol. The good performance of hybrid meta-GGAs confirms the usefulness of including kinetic energy densities to obtain a balanced treatment of exchange and correlation. However, it is disappointing that functionals that work well for the catalysis database do not yield good results for spin-splitting. New functionals need to be developed with improved performance for spin splitting, while retaining good performance for main-group thermochemistry, barrier heights, transition metal chemistry, and noncovalent interactions.

In contrast to the results with ΔSCF and low-spin time-dependent DFT methods, the collinear spin-flip time-dependent DFT method yields good results for both valence and Rydberg multiplicity changing excitations only when the percentage of Hartree–Fock exchange is rather high, about 60%. The direct comparisons in this paper provide an important reminder that the performance of a density functional for excited states depends not just on the density functional but also on the DFT formalism used to calculate the excited-state energy.

Almost perfect linear dependence of the calculated excitation energies on the percentage of HF exchange has been observed for the B3LYP*X* series of functionals. The optimum value of *X* is both system-dependent and method-dependent. Without changing the functional form, one cannot find an optimum percentage of HF exchange for the excitation energies in general.

ACKNOWLEDGMENTS

The authors are grateful to Dr. Boris Averkiev for creating the experimental database. Valuable discussions with Boris Averkiev and Sijie Luo are gratefully acknowledged. This work was supported in part by the National Science Foundation under Grant No. CHE09-56776 and by the Air Force Office of Scientific Research.

[1] P. Hohenberg and W. Kohn, Phys. Rev. **136**, B864 (1964).
[2] W. Kohn and L. J. Sham, Phys. Rev. **140**, A1133 (1965).
[3] C. J. Cramer and D. G. Truhlar, Phys. Chem. Chem. Phys. **11**, 10757 (2009).
[4] T. Ziegler, A. Rauk, and E. J. Baerends, Theor. Chim. Acta **43**, 261 (1977).
[5] U. von Barth, Phys. Rev. A **20**, 1693 (1979).
[6] T. Ziegler, Chem. Rev. **91**, 651 (1991).
[7] O. Gunnarsson and B. I. Lundqvist, Phys. Rev. B **13**, 4247 (1976).
[8] E. Runge and E. K. U. Gross, Phys. Rev. Lett. **52**, 997 (1984).
[9] M. Petersilka, U. J. Grossman, and E. K. U. Gross, Phys. Rev. Lett. **76**, 1212 (1996).
[10] R. Bauernschmitt and R. Ahlrichs, Chem. Phys. Lett. **256**, 454 (1996).
[11] R. E. Stratmann, G. E. Scuseria, and M. J. Frisch, J. Chem. Phys. **109**, 8218 (1998).
[12] M. A. L. Marques and E. K. U. Gross, Annu. Rev. Phys. Chem. **55**, 427 (2004).
[13] A. Dreuw and M. Head-Gordon, Chem. Rev. **105**, 4009 (2005).
[14] R. van Leeuwen, Int. J. Mod. Phys. B **15**, 1969 (2001).
[15] J. Schirmer and A. Dreuw, Phys. Rev. A **78**, 056502 (2008).
[16] T. A. Niehaus and N. H. March, Theor. Chem. Acc. **125**, 427 (2009).
[17] A. D. McLachlan and M. A. Ball, Rev. Mod. Phys. **36**, 844 (1964).
[18] D. Jacquemin, E. A. Perpete, I. Ciofini, and C. Adamo, J. Chem. Theory Comput. **6**, 1532 (2010).
[19] Y. Shao, M. Head-Gordon, and A. I. Krylov, J. Chem. Phys. **118**, 4807 (2003).
[20] F. Wang and T. Ziegler, J. Chem. Phys. **121**, 12191 (2004).
[21] A. I. Krylov, J. Phys. Chem. A **109**, 10638 (2005), and references therein.
[22] M. E. Casida, in *Recent Advances in Density Functional Methods, Part I*, edited by D. P. Chong (World Scientific, Singapore, 1995), p. 155.
[23] B. G. Levine, C. Ko, J. Quenneville, and T. J. Martínez, Mol. Phys. **104**, 1039, (2006).
[24] Z. Rinkevicius, O. Vahtras, and H. Ågren, J. Chem. Phys. **133**, 114104 (2010).
[25] Y. Jung and M. Head-Gordon, J. Phys. Chem. A **107**, 7475 (2003).
[26] Y. Jung and M. Head-Gordon, ChemPhysChem **4**, 522 (2003).

[27] Y. Jung, T. Heine, P. v. R. Schleyer, and M. Head-Gordon, J. Am. Chem. Soc. **126**, 3132 (2004).
[28] Y. Jung, M. Brynda, P. P. Power, and M. Head-Gordon, J. Am. Chem. Soc. **128**, 7185 (2006).
[29] A. de la Lande, V. Moliner, and O. Parisel, J. Chem. Phys. **126**, 035102 (2007).
[30] A. de la Lande, H. Gerard, and O. Parisel, Int. J. Quantum Chem. **108**, 1898 (2008).
[31] A. de la Lande, O. Parisel, H. Gerard, V. Moliner, and O. Reinaud, Chem. Eur. J. **14**, 6465 (2008).
[32] A. de la Lande, D. Salahub, V. Moliner, H. Gerard, J.-P. Piquemal, and O. Parisel, Inorg. Chem. **48**, 7003 (2009).
[33] N. Minezawa and M. S. Gordon, J. Phys. Chem. A **113**, 12749 (2009).
[34] M. Huix-Rotllant, B. Natarajan, A. Ipatov, C. M. Wawire, T. Deutsch, and M. E. Casida, Phys. Chem. Chem. Phys. **12**, 12811 (2010).
[35] Z.-Q. You, Y. Shao, and C. P. Hsu, Chem. Phys. Lett. **390**, 116 (2004).
[36] C. H. Yang and C. P. Hsu, J. Chem. Phys. **124**, 244507 (2006).
[37] W. Zhang, W. Zhu, W. Liang, Y. Zhao, and S. F. Nelsen, J. Phys. Chem. B **112**, 11079 (2008).
[38] D. W. Keogh and R. Poli, J. Am. Chem. Soc. **119**, 2516 (1997).
[39] D. Schroder, S. Shaik, and H. Schwarz, Acc. Chem. Res. **33**, 139 (2000).
[40] Top. Curr. Chem., edited by P. Gutlich and H. A. Goodwin (Springer, Berlin, 2004), Vols. 233-235.
[41] M. Hustettler, K. W. Törnroos, D. Chernyshov, and B. Vangdai, Angew. Chem. Int. Ed. **43**, 4589 (2004).
[42] C. Enachescu, A. Hauser, J.-J. Girerd, and M.-L. Boillot, ChemPhysChem **7**, 1127 (2006).
[43] M. Reiher, Chimia **63**, 140 (2009).
[44] M. Reiher, O. Salomon, and B. A. Hess, Theor. Chem. Acc. **107**, 48 (2001).
[45] M. Reiher, Inorg. Chem. **41**, 6928 (2002).
[46] A. Fouqueau, S. Mer, M. E. Casida, L. M. L. Daku, A. Hauser, T. Mineva, and F. Neese, J. Chem. Phys. **120**, 9473 (2004).
[47] A. Fouqueau, M. E. Casida, L. M. L. Daku, A. Hauser, and F. Neese, J. Chem. Phys. **120**, 044110 (2004).
[48] L. M. L. Daku, A. Vargas, A. Hauser, A. Fouqueau, and M. E. Casida, ChemPhysChem **6**, 1393 (2005).
[49] R. J. Deeth and N. Fey, J. Comput. Chem. **25**, 1840 (2004).
[50] M. Swart, A. R. Groenhof, A. W. Ehlers, and K. Lammertsma, J. Phys. Chem. A **108**, 5479 (2004).
[51] G. Ganzenmuller, N. Berkaine, A. Fouqueau, M. E. Casida, and M. Reiher, J. Chem. Phys. **122**, 234321 (2005).
[52] J. Conradie and A. Ghosh, J. Chem. Theory Comput. **3**, 689 (2007).
[53] K. Pierloot and S. Vancoillie, J. Chem. Phys. **125**, 124303 (2006).
[54] K. Pierloot and S. Vancoillie, J. Chem. Phys. **128**, 034104 (2008).
[55] M. Guell, J. M. Luis, M. Sola, and M. Swart, J. Phys. Chem. A **112**, 6384 (2008).
[56] M. Kepenekian, V. Robert, B. Le Guennic, and C. De Graaf, J. Comput. Chem. **30**, 2327 (2009).
[57] S. Vancoillie, H. Zhao, M. Radon, and K. Pierloot, J. Chem. Theory Comput. **6**, 576 (2010).
[58] K. P. Jensen and J. Cirera, J. Phys. Chem. A **113**, 10033 (2009).
[59] N. C. Handy and A. J. Cohen, Mol. Phys. **99**, 403 (2001).
[60] J. P. Perdew, K. Burke, and M. Ernzerhof, Phys. Rev. Lett. **77**, 3865 (1996).
[61] C. Lee, W. Yang, and R. G. Parr, Phys. Rev. B **37**, 785 (1988).
[62] V. N. Staroverov, G. E. Scuseria, J. Tao, and J. P. Perdew, J. Chem. Phys. **119**, 12129 (2003); *ibid* **121**, 11507 (2004).
[63] F. Neese, Coord. Chem. Rev. **253**, 526 (2009).
[64] L. Noodleman, J. Chem. Phys. **74**, 5737 (1981).
[65] M. Nishino, S. Yamanaka, Y. Yoshioka, and K. Yamaguchi, J. Phys. Chem. A **101**, 705 (1997).
[66] E. Ruiz, J. Cano, S. Alvarez, and P. Alemany, J. Comput. Chem. **20**, 1391 (1999).
[67] R. Valero, R. Costa, I. d., P. R. Moreira, D. G. Truhlar, and F. IIIas, J. Chem. Phys. **128**, 114103 (2008).
[68] I. Rudra, Q. Wu, and T. Van Voorhis, J. Chem. Phys. **124**, 024103 (2006).
[69] K. Andersson, P. A. Malmqvist, B. O. Roos, A. J. Sadlej, and K. Wolinski, J. Phys. Chem. **94**, 5483 (1990).
[70] K. Andersson, P. A. Malmqvist, and B. O. Roos, J. Chem. Phys. **96**, 1218 (1992).
[71] J. C. Slater, in *Quantum Theory of Molecules and Solids* (McGraw-Hill, New York, 1974), Vol. 4.
[72] J. P. Perdew and A. Zunger, Phys. Rev. B **23**, 5048 (1981).
[73] J. P. Perdew and Y. Wang, Phys. Rev. B **45**, 13244 (1992).
[74] S. H. Vosko, L. Wilk, and M. Nusair, Can. J. Phys. **58**, 1200 (1980).
[75] A. D. Becke, Phys. Rev. A **38**, 3098 (1988).
[76] J. P. Perdew, in *Electronic Structure of Solids '91*, edited by P. Ziesche and H. Esching (Akademie Verlag, Berlin, 1991), p. 11.
[77] N. E. Schultz, Y. Zhao, and D. G. Truhlar, J. Phys. Chem. A **109**, 11127 (2005).
[78] C. Adamo and V. Barone, J. Chem. Phys. **108**, 664 (1998).
[79] B. Hammer, L. B. Hansen, and J. K. Nørskov, Phys. Rev. B **59**, 7413 (1999).
[80] P. J. Stephens, F. J. Devlin, C. F. Chabalowski, and M. J. Frisch, J. Phys. Chem. **98**, 11623 (1994).
[81] A. D. Becke, J. Chem. Phys. **98**, 5648 (1993).
[82] R. H. Hertwig and W. Koch, Chem. Phys. Lett. **268**, 345 (1997).
[83] T. W. Keal and D. J. Tozer, J. Chem. Phys. **123**, 121103 (2005).
[84] H. L. Schmider and A. D. Becke, J. Chem. Phys. **108**, 9624 (1998).
[85] B. J. Lynch, P. L. Fast, M. Harris, and D. G. Truhlar, J. Phys. Chem. A **104**, 4811 (2000).
[86] Y. Zhao and D. G. Truhlar, J. Phys. Chem. A **108**, 6908 (2004).
[87] W. M. Hoe, A. J. Cohen, and N. C. Handy, Chem. Phys. Lett. **341**, 319 (2001).
[88] C. Adamo and V. Barone, J. Chem. Phys. **110**, 6158 (1999).
[89] T. Yanai, D. P. Tew, and N. C. Handy, Chem. Phys. Lett. **393**, 51 (2004).
[90] J. Heyd, G. E. Scuseria, and M. Ernzehof, J. Chem. Phys. **118**, 8207 (2003); *ibid* **124**, 219906 (2006).
[91] T. M. Henderson, A. F. Izmaylov, G. Scalmani, and G. E. Scuseria, J. Chem. Phys. **131**, 044108 (2009).
[92] H. Iikura, T. Tsuneda, T. Yanai, and K. Hirao, J. Chem. Phys. **115**, 3540 (2001).
[93] O. V. Vydrov and G. E. Scuseria, J. Chem. Phys. **125**, 234109 (2006).
[94] J. Chai and M. Head-Gordon, J. Chem. Phys. **128**, 084106 (2008).
[95] J. Chai and M. Head-Gordon, Phys. Chem. Chem. Phys. **10**, 6615 (2008).
[96] Y. Zhao and D. G. Truhlar, J. Chem. Phys. **125**, 194101 (2006).
[97] J. Tao, J. P. Perdew, V. N. Staroverov, and G. E. Scuseria, Phys. Rev. Lett. **91**, 146401 (2003).
[98] T. Van Voorhis and G. E. Scuseria, J. Chem. Phys. **109**, 400 (1998).
[99] A. D. Boese and J. M. L. Martin, J. Chem. Phys. **121**, 3405 (2004).
[100] Y. Zhao, N. E. Schultz, and D. G. Truhlar, J. Chem. Phys. **123**, 161103 (2005).
[101] Y. Zhao, N. E. Schultz, and D. G. Truhlar, J. Chem. Theory Comput. **2**, 364 (2006).
[102] Y. Zhao and D. G. Truhlar, Theor. Chem. Acc. **120**, 215 (2008).
[103] Y. Zhao and D. G. Truhlar, J. Phys. Chem. A **110**, 13126 (2006).
[104] Y. Zhao and D. G. Truhlar, J. Chem. Theory Comput. **4**, 1849 (2008).
[105] J. B. Krieger, J. Chen, G. J. Iafrate, and A. Savin, in *Electron Correlations and Materials Properties*, edited by A. Gonis, and N. Kioussis (Plenum, New York, 1999), p. 463.
[106] Y. Zhao, N. González-García, and D. G. Truhlar, J. Phys. Chem. A **109**, 2012 (2005).
[107] Y. Zhao and D. G. Truhlar, J. Phys. Chem. A **109**, 5656 (2005).
[108] Y. Zhao, B. J. Lynch, and D. G. Truhlar, Phys. Chem. Chem. Phys. **7**, 43 (2005).
[109] A. D. Boese and N. C. Handy, J. Chem. Phys. **116**, 9559 (2002).
[110] K. Yang, J. Zheng, Y. Zhao, and D. G. Truhlar, J. Chem. Phys. **132**, 164117 (2010).
[111] A. Savin, in *Recent Developments and Applications of Modern Density Functional Theory*, edited by J. Seminario (Elsevier, Amsterdam, 1996), p. 327.
[112] Y. Tawada, T. Tsuneda, S. Yanagisawa, T. Yanai, and K. Hirao, J. Chem. Phys. **120**, 8425 (2004).
[113] P. M. W. Gill, R. D. Adamson, and J. A. Pople, Mol. Phys. **88**, 1005 (1996).
[114] M. Ernzerhof and J. P. Perdew, J. Chem. Phys. **109**, 3313 (1998).
[115] M. J. G. Peach, P. Benfield, T. Helgaker, and D. J. Tozer, J. Chem. Phys. **128**, 044118 (2008).
[116] L Goerigk and S. Grimme, J. Chem. Theory Comput. **7**, 291 (2011).
[117] Y. Zhao and D. G. Truhlar, Acc. Chem. Res. **41**, 157 (2008).
[118] Y. Zhao and D. G. Truhlar, Rev. Mineral. Geochem. **71**, 19 (2010).
[119] Y. Zhao and D. G. Truhlar, Chem. Phys. Lett. **502**, 1 (2011).
[120] R. Li, J. Zhang, and D. G. Truhlar, Phys. Chem. Chem. Phys. **12**, 12697 (2010).
[121] C. E. Moore, *Atomic Energy Levels*, Vol. I–II, Circular of the National Bureau of Standards 467, U.S. Government Printing Office, Washington, DC (1949).

[122]M. J. Frisch, G. W. Trucks, H. B. Schlegel *et al.*, GAUSSIAN03, Gaussian, Inc., Pittsburgh, PA, 2003, Y. Zhao and D. G. Truhlar, MN-GFM, versions 4.2 and 4.3, University of Minnesota, Minneapolis, 2009.
[123]M. J. Frisch, G. W. Trucks, H. B. Schlegel *et al.*, GAUSSIAN09, Revision A.1, Gaussian, Inc., Wallingford, CT, 2009.
[124]R. Seeger and J. A. Pople, J. Chem. Phys. **66**, 3045 (1977).
[125]R. Bauernschmitt and R. Ahlrichs, J. Chem. Phys. **104**, 9047 (1996).
[126]T. H. Dunning, Jr., J. Chem. Phys. **90**, 1007 (1989).
[127]D. E. Woon and T. H. Dunning, Jr., J. Chem. Phys. **98**, 1358 (1993).
[128]A. K. Wilson, D. E. Woon, K. A. Peterson, and T. H. Dunning, Jr., J. Chem. Phys. **110**, 7667 (1999).
[129]F. Weigend and R. Ahlrichs, Phys. Chem. Chem. Phys. **7**, 3297 (2005).
[130]D. E. Woon and T. H. Dunning, Jr., J. Chem. Phys. **100**, 2975 (1993).
[131]J. Zheng, X. Xu, and D. G. Truhlar, Theor. Chem. Acc. **128**, 295 (2010).
[132]M. Douglas and N. M. Kroll, Ann. Phys. **82**, 89 (1974).
[133]B. A. Hess, Phys. Rev. A **33**, 3742 (1986).
[134]G. Jansen and B. A. Hess, Phys. Rev. A **39**, 6016.
[135]W. A. de Jong, R. J. Harrison, and D. A. Dixon, J. Chem. Phys. **114**, 48 (2001).
[136]J. A. Pople, M. Head-Gordon, and K. Raghavachari, J. Chem. Phys. **87**, 5968 (1987).
[137]Y. Shao, L. Fusti-Molnar, Y. Jung, J. Kussmann, C. Ochsenfeld, S. T. Brown, A. T. B. Gilbert, L. V. Slipchenko, S. V. Levchenko, D. P. O'Neill, R. A. Distasio, Jr., R. C. Lochan, T. Wang, G. J. O. Beran, N. A. Beasley, J. M. Herbert, C. Y. Lin, T. Van Voorhis, S. H. Chien, A. Sodt, R. P. Steele, V. A. Rassolov, P. E. Maslen, P. P. Korambath, R. D. Adamson, B. Austin, J. Baker, E. F. C. Byrd, H. Dachsel, R. J. Doerksen, A. Dreuw, B. D. Dunietz, A. D. Dutoi, T. R. Furlani, S. R. Gwaltney, A. Heyden, S. Hirata, C.-P. Hsu, G. Kedziora, R. Z. Khaliullin, P. Klunzinger, A. M. Lee, M. S. Lee, W. Liang, I. Lotan, N. Nair, B. Peters, E. I. Proynov, P. A. Pieniazek, Y. M. Rhee, J. Ritchie, E. Rosta, C. D. Sherrill, A. C. Simmonett, J. E. Subotnik, H. L. WoodcockIII, W. Zhang, A. T. Bell, A. K. Chakraborty, D. M. Chipman, F. J. Keil, A. Warshel, W. J. Hehre, H. F. Schaefer III, J. Kong, A. I. Krylov, P. M. W. Gill, and M. Head-Gordon, Phys. Chem. Chem. Phys. **8**, 3172 (2006).
[138]I. Tamm, J. Phys. (Moscow) **9**, 449 (1945).
[139]S. Hirata and M. Head-Gordon, Chem. Phys. Lett. **314**, 291 (1999).
[140]I. Ciofini and C. Adamo, J. Phys. Chem. A **111**, 5549 (2007).
[141]Z. Cai, D. J. Tozer, and J. R. Reimers, J. Chem. Phys. **113**, 7084 (2000).
[142]Q. Wu, A. J. Cohen, and W. Yang, Mol. Phys. **103**, 711 (2005).
[143]M. J. G. Peach, P. Benfield, T. Helgaker, and D. J. Tozer, J. Chem. Phys. **128**, 044118 (2008).
[144]M. E. Casida, C. Jamorski, K. C. Casida, and D. R. Salahub, J. Chem. Phys. **108**, 4439 (1998).
[145]N. A. Besley, A. T. B. Gilbert, and P. M. W. Gill, J. Chem. Phys. **130**, 124308 (2009).
[146]O. V. Gritsenko, P. R. T. Schipper, and E. J. Baerends, Chem. Phys. Lett. **302**, 199 (1999).
[147]P. R. T. Schipper, O. V. Gritsenko, S. J. A. van Gisbergen, and E. J. Baerends, J. Chem. Phys. **112**, 1344 (2000).
[148]M. Grüning, O. V. Gritsenko, S. J. A. van Gisbergen, and E. J. Baerends, J. Chem. Phys. **116**, 9591 (2002).
[149]C. Hu, O. Sugino, and Y. Miyamoto, Phys. Rev. A **74**, 032508 (2006).
[150]C. Hu, O. Sugino, and Y. Tateyama, J. Phys. Condens. Matter **21**, 064229 (2009).
[151]G. Cui and W. Yang, Mol. Phys. **108**, 2745 (2010).
[152]A. Dreuw and M. Head-Gordon, J. Am. Chem. Soc. **126**, 4007 (2004).
[153]T. Ziegler, M. Seth, M. Krykunov, J. Autschbach, and F. Wang, J. Chem. Phys. **130**, 154102 (2009).
[154]T. Ziegler, M. Seth, M. Krykunov, J. Autschbach, and F. Wang, J. Mol. Phys.: THEOCHEM **914**, 106 (2009).
[155]T. Ziegler and M. Krykunov, J. Chem. Phys. **133**, 074104 (2010).
[156]F. Wang and T. Ziegler, J. Chem. Phys. **122**, 074109 (2005).
[157]A. Ipatov, F. Cordova, L. J. Doriol, and M. E. Casida, J. Mol. Struct.: THEOCHEM **914**, 60 (2009).
[158]A. I. Krylov, Chem. Phys. Lett. **338**, 375 (2001).
[159]O. Vahtras and Z. Rinkevicius, J. Chem. Phys. **126**, 114101 (2007).
[160]Z. Li and W. Liu, J. Chem. Phys. **133**, 064106 (2010).
[161]Z. Li, W. Liu, Y. Zhang, and B. Suo, J. Chem. Phys. **134**, 134101 (2011).
[162]F. Wang and T. Ziegler, J. Chem. Phys. **122**, 074109 (2005).
[163]Z. Rinkevicius and H. Ågren, Chem. Phys. Lett. **491**, 132 (2010).
[164]See supplementary material at http://dx.doi.org/10.1063/1.3607312 for additional details. The supplementary material includes ΔSCF, LS-TDDFT, and SF-TDDFT results with additional basis sets. The mean absolute deviations (MADs) of post-SCF and SCF calculated excitation energies, full sets of coupled cluster results, and the full version of Figs. 3 and 4 with all tested functionals are also listed in the supplementary material.
[165]B. J. Lynch and D. G. Truhlar, J. Phys. Chem. A **107**, 8996 (2003).
[166]J. Zheng, Y. Zhao, and D. G. Truhlar, J. Chem. Theory. Comput. **3**, 569 (2007).
[167]J. Zheng, Y. Zhao, and D. G. Truhlar, J. Chem. Theory, Comput. **5**, 808 (2009).